Study of mechanisms for the axonal localization of the tau protein in neurons

Doctoral Dissertation

A thesis submitted for the degree of Doctor of Philosophy in Science

Minori Iwata

Supervisor:

Dr. Hiroaki Misono

Co-Supervisor:

Dr. Shoji Watanabe

Graduate School of Brain Science, Doshisha University

March 2020

Kyoto, Japan

ABSTRACT

Microtubule-associated protein tau localizes specifically to neuronal axons, where it is thought to play important roles in polymerization and stabilization of microtubules. Tau is also a cause of Tauopathies including Alzheimer's disease. In these disorders, tau is accumulated in the soma and dendrites and forms neurofibrillary tangles. Therefore, it is speculated that the disruption of axonal localization precedes and causes the somatodendritic accumulation of tau. However, the molecular mechanism of axonal localization, as well as how it is disrupted, remains elusive. Therefore, I started my study to elucidate the molecular mechanism of the axon localization of tau.

When tau is constantly overexpressed in cultured neurons using conventional transfection, the expressed tau is localized not only in the axons but also in the soma and dendrites. Therefore, I needed to establish an experimental system that localizes exogenous tau in the axon to study the mechanism. I found that localization of endogenous tau to the axon is almost completed when the axon is first generated in immature neurons at early developmental stages. From this, I thought that it was necessary to follow the temporal profiles of expression of endogenous tau for exogenous tau to localize to the axon.

Using a lentiviral vector and an inducible expression strategy, I established an experimental system which expresses exogenous tau transiently in immature neurons in culture. Interestingly, exogenous tau expressed at 1 day in culture for 1 h with this system localized specifically to the axon. With this new experimental model, regions required for the axonal localization was determined using deletion mutants. I found that the proline rich region 2 (PRR2), which contains important phosphorylation sites and is known to participate in microtubule-binding, is critical for the localization. Surprisingly, the deletion of the microtubule-binding domain (MTBD) did not affect the axonal localization. Fluorescence recovery after photobleaching (FRAP) experiments confirmed the lack of microtubule binding of this mutant. These results suggest that stable binding to microtubules is not necessary for the localization.

Tau has been shown as a cargo of the slow axonal transport. Therefore, the mis-localization of tau lacking PRR2 (ΔPRR2) may be due to either tight MT-binding or the disruption of tau transport to the axon. To investigated these possibilities, I performed FRAP for ΔPRR2. ΔPRR2 showed reduced MT-binding. I was able to detect directional anterograde transport of wild-type tau to the axon and found that the deletion of PRR2 disrupted this transport.

Further experiments provided evidence that phosphorylation of PRR2 regulates microtubule-binding and axonal localization. Dephosphorylation-mimetic mutant showed tight microtubule-binding but mis-localized to the soma and dendrites. These results suggest that stable microtubule-binding is not necessary, and that tau needs to be liberated from microtubules to be transported into the axon. Phosphorylation-mimetic mutant showed reduced microtubule-binding. However, this mutant also mis-localized to the soma and dendrites. The changes were similar to those by the PRR2 deletion. Therefore, I speculated that transport of tau to the axon may be affected by PRR2 phosphorylation.

This research provides novel findings regarding mechanisms for the axonal localization of tau and regulation by phosphorylation and microtubule-binding using the method that specifically localizes exogenous tau to axons in neurons. I believe that the results contribute greatly to the study of tau in normal and in the pathology of Alzheimer's disease.

ACKNOWLEDGEMENT

I would like to express my deepest gratitude to Dr. Hiroaki Misono for providing me with a place for continuous guidance and research. I would also like to express my gratitude to Dr. Shoji Watanabe for his precise comments and technical teaching. I would like to thank Dr. Moritoshi Hirono for his helpful comments.

I would like to express my gratitude to Dr. Tomohiro Miyasaka. This research could not have been completed without his support.

I would like to thank Dr. Nobuyuki Nukina, Dr. Tomoyuki Yamanaka, Dr. Haruko Miyazaki, and Dr. Naoto Saitoh for confocal microscopy, Dr. Shigeo Takamori and Dr. Yoshihiro Egashira for their technical assistance in lentivirus preparation.

I am grateful to my thesis committee Dr. Jun Motoyama, Dr. Nobuyuki Nukina and Dr. Shigeo Takamori for their insightful comments and encouragement.

Special thanks to Dr. Kohta Kobayasi and senior of his lab for their spiritually support.

I am deeply grateful to all the professors, the lab members, graduate students and friends who involved my study. I would like to offer my special thanks to my family for understanding and encouragement for everything.

TABLE OF CONTENTS

LIST OF FIGURES AND TABLES

1. INTRODUCTION

Neuronal cells are large and complex cells with long axons and highly branched dendrites, which serve as their input and output devices and underpin neuron's computational abilities. These long and fine structures are supported by a number of cytoskeletal structures, and particularly by microtubules (MTs), which distribute throughout neurons in the soma, dendrites, and the axon (**Fig. 1**).

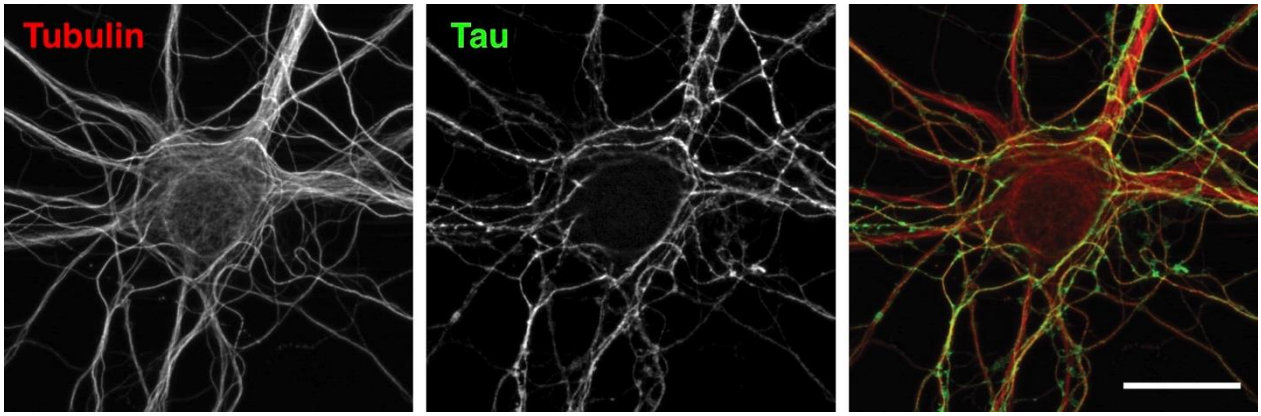

Fig. 1. **Distribution of α-tubulin and tau in cultured hippocampal neurons.**
Tubulin antibody (DM1A, red) labels fibrous microtubules in the soma, dendrites, and the axon. In contrast, tau (Anti-TauN, green) is absent from the soma and dendrites and found only in the axon in mature cultured neurons. Scale bar, 20 μm.

MTs in these structures are thought to be stabilized by a number of binding proteins called microtubule-associated proteins or MAPs. Tau is one of the MAPs and specifically localized to the axon and bound to the axonal MTs (Kubo et al., 2019a) (**Figs. 1 and 2**). In addition, tau is known for its pathological accumulation in neurons affected in Alzheimer's disease (AD). The abnormally accumulated tau is highly phosphorylated at various serine or threonine residues. Studies have identified potential protein kinases, which regulate tau phosphorylation, including GSK-3β (J. Avila, 2008).

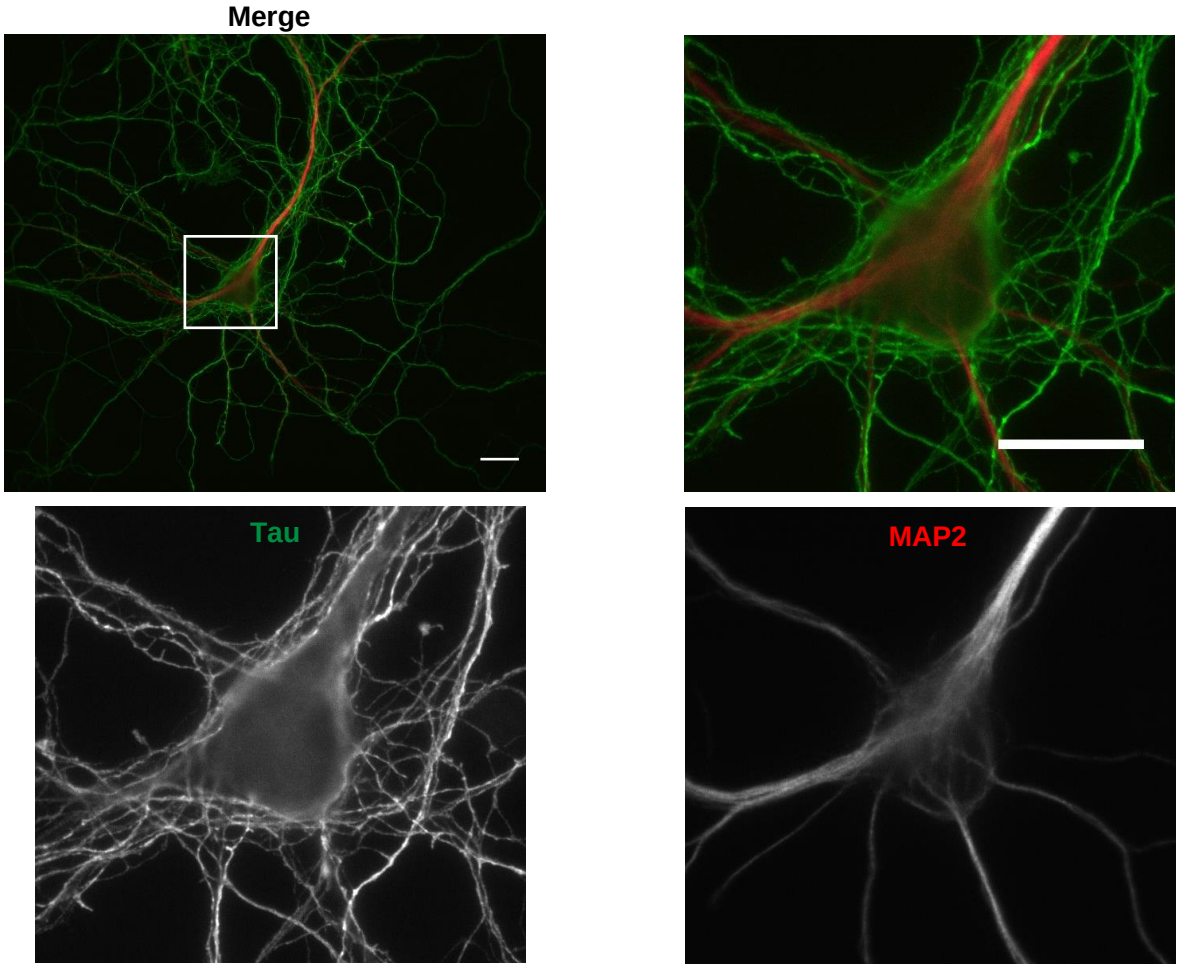

Fig. 2. **The localization of tau in cultured hippocampal neurons**

Tau (RTM38, green) localizes to the axon. In contrast, MAP2 (Anti-MAP2, red) localizes to dendrites and the soma. These proteins are both microtubule-associated proteins but show different localization. Scale bar: 20 μm.

Interestingly, tau accumulates mainly in the cell body and dendrites in AD (**Fig. 3**), although axonal tau inclusions have also been suggested as a subset of dystrophic neurites surrounding senile plaques (Tourtellotte and Van Hoesen, 1991; Kneynsberg et al., 2017; Ono et al., 2017). This suggests that tau loses the axon-specific localization during the pathogenesis. To understand how this occurs, I studied mechanisms for the axonal localization of tau, which would provide us what goes wrong in AD in my thesis research.

Fig. 3. **Somatodendritic neurofibrillary tangles in Alzheimer's disease**
Tau is accumulated in the soma and dendrites and forms neurofibrillary tangles in AD. The image shows tangles labeled with Bielshowsky staining of AD patient cortex. Image from Dr. Miyasaka.

1.1. Tau protein in neurodegenerative disorders.

AD accounts for the majority of progressive cognitive impairment in elderly populations, and AD patients are anticipated to grow in the general population (Cummings, 2002). There are two pathological hallmarks in AD, senile plaques and neurofibrillary tangles (**Fig. 3**). Senile plaques are composed mainly of β-amyloid, and tangles are fibrous aggregates of tau that is highly phosphorylated. From the analyses of postmortem brains, it is clearly shown that senile plaque

formation precedes the formation of neurofibrillary tangles by 10 to 20 years. This led to the dominant hypothesis in the research field, the amyloid cascade hypothesis, which states that toxic β-amyloid accumulation causes tau accumulation, neuronal dysfunction, and neurodegeneration. However, it is the neurofibrillary tangles, which are unambiguously linked to neuronal dysfunction and neurodegeneration from pathological and genetic evidence (Gómez-Isla et al., 1997; Delacourte et al., 1999; Ghetti et al., 2015). Neurofibrillary tangles are found only in patients' neurons, whereas normal subject brains can have substantial amount of senile plaques without any symptoms. Mutations in the tau gene have also been identified in the frontotemporal dementia with Parkinsonism 17 (FTDP-17) (Ghetti et al., 2015). From these findings, and the failures of a number of clinical trials of amyloid-targeted therapeutics, tau has accumulated considerable attention in the research field as an alternative therapeutic target.

As mentioned above, tau is normally localized to the neuronal axon (Kubo et al., 2019a). However, bulk of tau is accumulated in the cell body and dendrites as hyperphosphorylated forms in AD. I believe that understanding this mis-localization is a key to understand the pathogenesis of AD. Also, this mis-localization may be prerequisite for tau to cause synaptic dysfunction, which has been recently proposed as an early pathological step before tangle formation and neurodegeneration (Decker et al., 2015). Unfortunately, due to the lack of antibodies sensitive enough to detect normal unaggregated tau, the temporal relationship of tau mis-localization with hyper-phosphorylation and aggregation has not been elucidated. However, recent studies analyzing AD animal models suggested that mis-localization is necessary for the development of the other tau pathology (Kubo et al., 2019b). Therefore, it is important to understand how tau mis-localizes to the soma and dendrites, which may ultimately cause hyper-phosphorylation, tangle formation, and somatodendritic dysfunction of neurons in AD.

1.2. Physiology of tau protein in neurons

To understand how tau mis-localizes, we need to gain insights into how tau localizes to the axon. Here, I first summarize how neurons develop axons and basic physiology of MTs, MAPs, and tau.

Neurons make several neurites at an early developmental stage. One of them begins to grow very quickly and eventually becomes the axon (Fig. 4, Tomba, 2016).

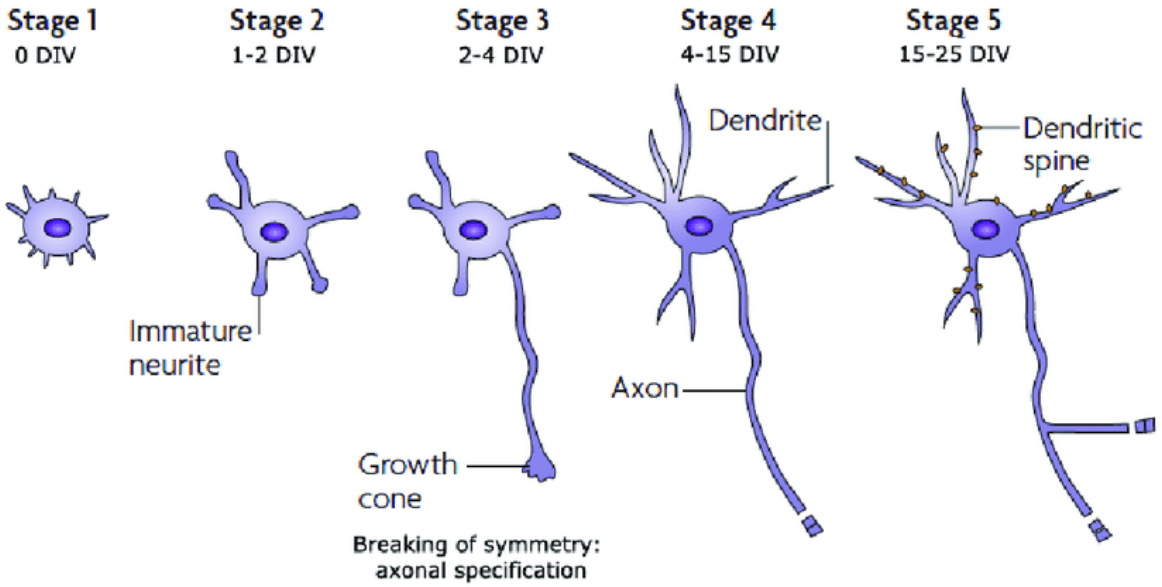

Fig. 4. **Developmental stages of neurons in culture**
There are defined neuronal developmental stages. Single axon is determined from a number of neurites, and the rest become dendrites. Illustration from Caterina Tomba, 2016. DIV is days in vitro.

It is thought that CRMP2, a member of the collapsin response mediator protein (CRMP) family, is involved in axon formation (Inagaki et al., 2001; Arimura and Kaibuchi 2007). CRMP2 is enriched in axons in stage 3 state. This overexpression has been shown to form and maintain multiple axons. In addition, this overexpression changes the dendrites at stage 4 of neurons into axons. Therefore, it is thought that it has an important role in axon formation and also a role in establishing neuronal polarity. The remaining neurites then grow and become dendrites (Dotti et al, 1988). Microtubule-associated protein TRIM46 (tripartite motif-containing protein 46) localizes to the proximal domain of the axon in polarized neurons. This protein is said to be involved in the identification of axon initial segment (AIS) and control of neuronal polarity (van Beuningen et al.,

2015; Curcio and Bradke, 2015). Knockdown of this protein changes tau localization in polarized neurons. This suggests that AIS is involved in maintaining tau after axonal localization. These developmental processes require intracellular transport systems, which is largely supported by MTs. MTs also maintain neuronal structures in mature neurons as well. MTs are composed of heterodimers consisting of one molecule each of α-tubulin and β-tubulin. Heterodimers polymerize at a fixed configuration. The side with β-tubulin is the plus end or growing end, and the opposite side with α-tubulin is called the minus end, where tubulins dissociate (**Fig. 5 (a)**, Valiron, 2001).

There are a number of MT-binding proteins identified, and they serve roles in MT polymerization, depolymerization, and stabilization (**Fig. 5 (b),** Voelzmann et al. 2016). The plus end binding proteins, or +TIPs, help MT polymerization, while the minus end binding proteins play a role in preventing depolymerization (Akhmanova and Hoogenraad, 2005). Unlike these binding proteins, tau binds to the shaft of MTs. It is categorized in the MAP2/Tau family and thought to play important roles in polymerization and stabilization of microtubules (Dehmelt and Halpain, 2004). This family is composed of MAP2, Tau, and MAP4. MAP2 and tau are expressed mainly in neurons, and MAP4 is found in various cell types in many different tissues. While MAP2 is restricted to the soma and dendrites, tau localizes to the axon in neurons. Because of their precise separation in neurons, these proteins have been widely used as marker proteins for their representing neuronal compartments.

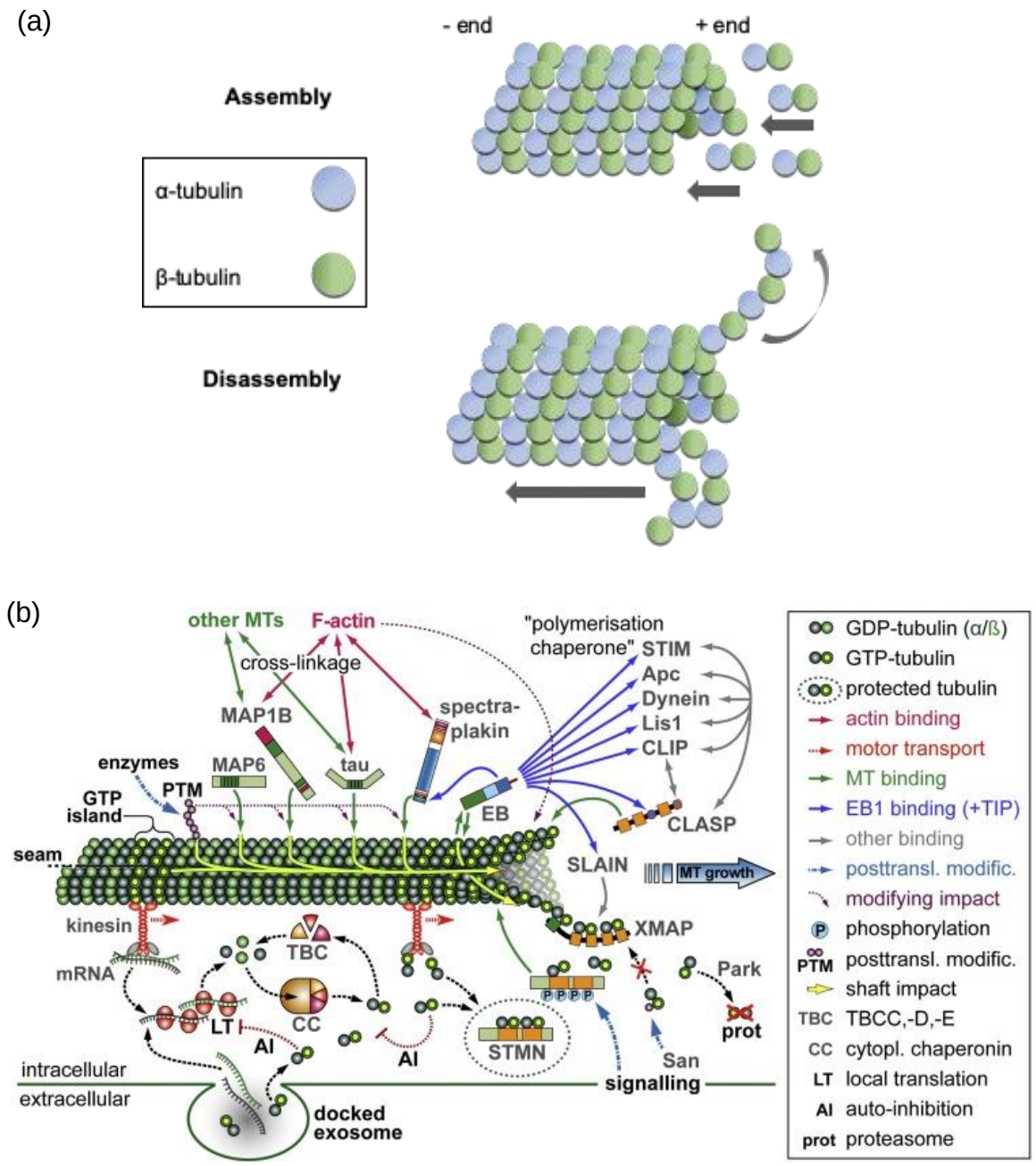

Fig. 5. **Structure and regulation of microtubules**

Microtubules (MTs) are composed of α-tubulin and β-tubulin heterodimers. β-tubulin side is called + end, and the assembly and disassembly occur on the + end side (a). There are a number of MT-binding proteins identified to date. Various aspects of MTs are controlled by them (b). Illustration in (b) from Voelzmann et al., 2016.

They share a common overall structure, in which there is a MT binding domain in the C-terminal half as three or four repeated sequences (**Fig. 6**). Tau has either 3 or 4 repeats depending on alternative splicing. In rodent, 3 repeat tau is expressed in early developmental stages and changes to 4 repeat tau in adult. Human neurons express 3 repeat tau in the fetal stage but have both 3 and 4 repeat tau in adult. Tau gene also contains two alternative splicing cassettes in the N-terminal region. Therefore, total of six isoforms can be generated. The N-terminal region has been shown to be involved in MT bundling activity. MT binding domain and the preceding region containing a number or proline residues, named proline-rich region or PRR, are important for MT-binding. PRR is also involved in the bundling activity (Kanai, 1992).

Tau has been considered to have a role to stabilize axonal MTs. Tau binds to MTs like paclitaxel, which is a well-known chemical reagent to stabilize microtubules. Also, the ability of tau to facilitate the polymerization and bundling of MTs in vitro supports this notion (Barbier et al., 2019). Recent studies found that knocking down tau in cultured neurons does not reduce the level of stable MTs but rather increases that of labile MTs (Quiang et al., 2018). Tau has also been implicated in neurite elongation and axonal trafficking (Mietelska-Porowska et al., 2014).

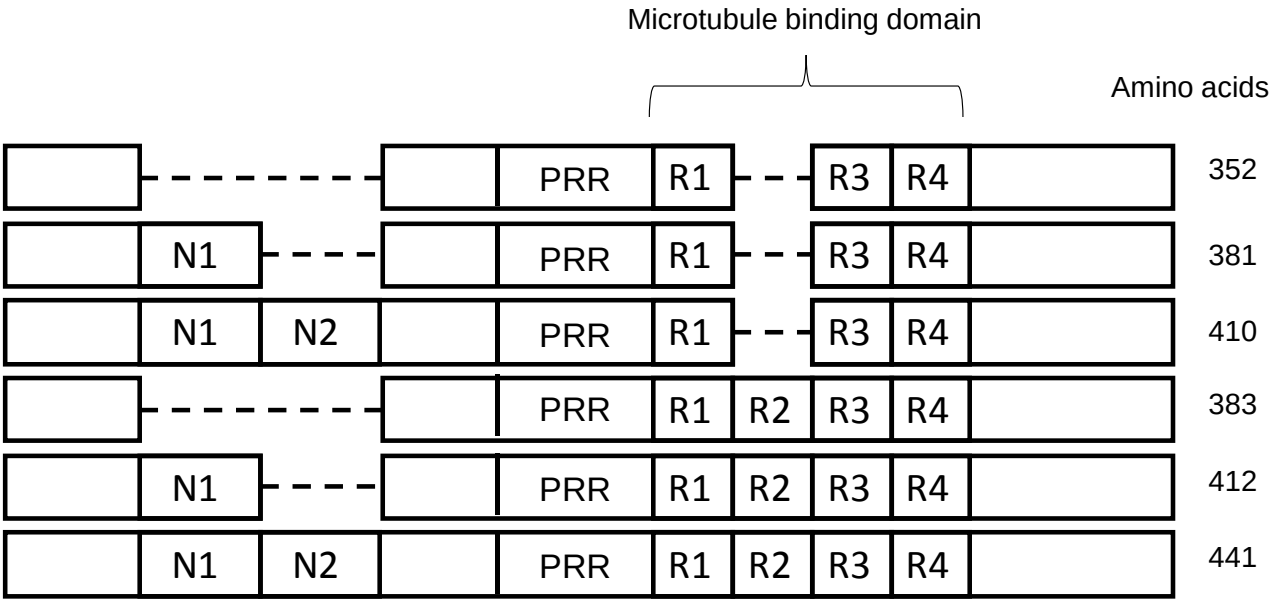

Fig.6. **Tau isoforms**

Tau have 6 isoforms. These are generated by alternative splicing.

1.3. Mechanisms for the axonal localization of tau

Previous studies have made considerable efforts to study and understand the mechanisms for the axonal localization of tau. Kanai and Hirokawa sought to identify the protein domain(s) required for the axonal localization of tau by injecting a series of tau deletion mutants into cultured neurons (Kanai and Hirokawa, 1992). They suggested that MT-binding of tau determined by the MT-binding domain is stronger in the axon than in dendrites, thereby localizing tau in the axon.

Tau has also been considered as a cytoplasmic protein that is transported by the slow axonal transport. Classic experiments with radioactive labeling of proteins in the peripheral nerve demonstrated that tau is a cargo of the slow component in the slow axonal transport (Tytell et al., 1984; Mercken et al., 1995; Tashiro et al., 1996). Recent advances in live-cell imaging allowed researchers to look into the intracellular trafficking of tau proteins in more details in neurons. These studies reported that tau is transported to the axon by MT- and motor protein-based mechanisms (Utton et al., 2005; Falzone et al., 2009; Scholz and Mandelkow, 2014). Mandelkow and colleagues also proposed a new hypothesis that tau can enter the axon freely but is prevented from exiting there. They reported that MT-based filter situated near or in the axon initial segment restricts tau from entering the soma while allowing it to go into the axon (Li et al., 2011). This is somewhat similar to the filter hypothesis that actin-based mechanisms prevent large cytoplasmic proteins to go through the axon initial segment (Song et al., 2009).

Although a number of studies have looked into these mechanisms, there had been two major problems in studying tau localization summarized below.

1.4. Problems in tau research and our approach

First, there were only a few good antibodies to detect unaggregated tau with enough sensitivity without hyperphosphorylation. There are a number of antibodies specific for phosphorylated and dephosphorylated tau at specific sites. But, antibodies that can detect total tau had been scarce. Presumably because of this, the localization of total tau in neurons in vivo and in culture has not

been reported. In fact, the axonal localization of tau has only been demonstrated with a dephosphorylation specific antibody, tau-1. My collaborator, Dr. Miyasaka, has generated a number of antibodies, which can sensitively and reliably detect tau regardless of the phosphorylation states (Kubo et al., 2019a). Using these antibodies, they reported for the first time that the majority of tau proteins is localized in the axon regardless of the phosphorylation state in cultured neurons and in the mouse brain.

Second, it had been difficult to localize tau expressed exogenously in neurons. When tau is constitutively expressed in cultured neurons by transfection, it typically distributes uniformly throughout the cells (Xia et al., 2016), such that the major population of tau remains in the soma and dendrites (see **Fig. 7**). This "mis-localization" makes it difficult to study axonal localization mechanisms of tau in a precise manner.

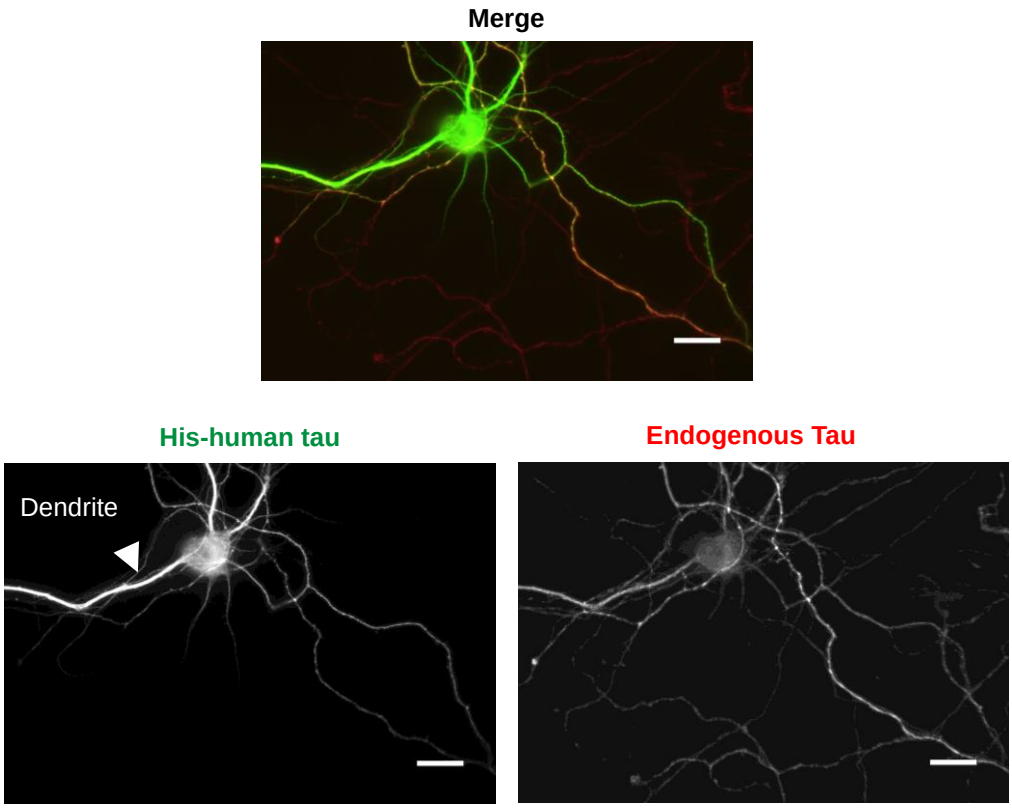

Fig. 7. Exogenous tau is distributed not only to the axon but also the soma and dendrites
Exogenous human tau with the His-tag (green) is retained in the soma and dendrites, when it is expressed constitutively by a CMV promoter. Human tau was transfected into neurons at 7 days in vitro (DIV). arrowhead is dendrite. Neurons were fixed at 9 DIV and immunostained for the His-tag and endogenous rat tau (rodent-tauN, red). Scale bar: 20 μm

In this thesis research, I set to tackle this challenge and establish a good experimental model for studying tau localization. I was able to establish an experimental model in which exogenous tau is expressed like endogenous tau and colocalizes with endogenous tau in the axon in both developing and mature neurons. With this model, I show novel findings on the relationship between MT-binding and axonal localization of tau, the involvement of the proline-rich region in tau localization, and how phosphorylation affects the localization and MT-binding. These results will be useful for studying the detailed mechanism of tau axon localization in the future. In addition, these results would provide new questions and hypotheses regarding how tau localizes to the axon and how it is disrupted in Alzheimer's disease.

2. MATERIALS AND METHODS

2.1. Primary culture of hippocampal neurons

Primary hippocampal neurons were used in this study. They need humoral factors from astrocytes to survive in culture. Therefore, they were co-cultured with primary astrocytes using the method developed by Banker and Goslin with modifications (**Fig. 8**) (Misonou et al., 2005, Kaech et al., 2006).

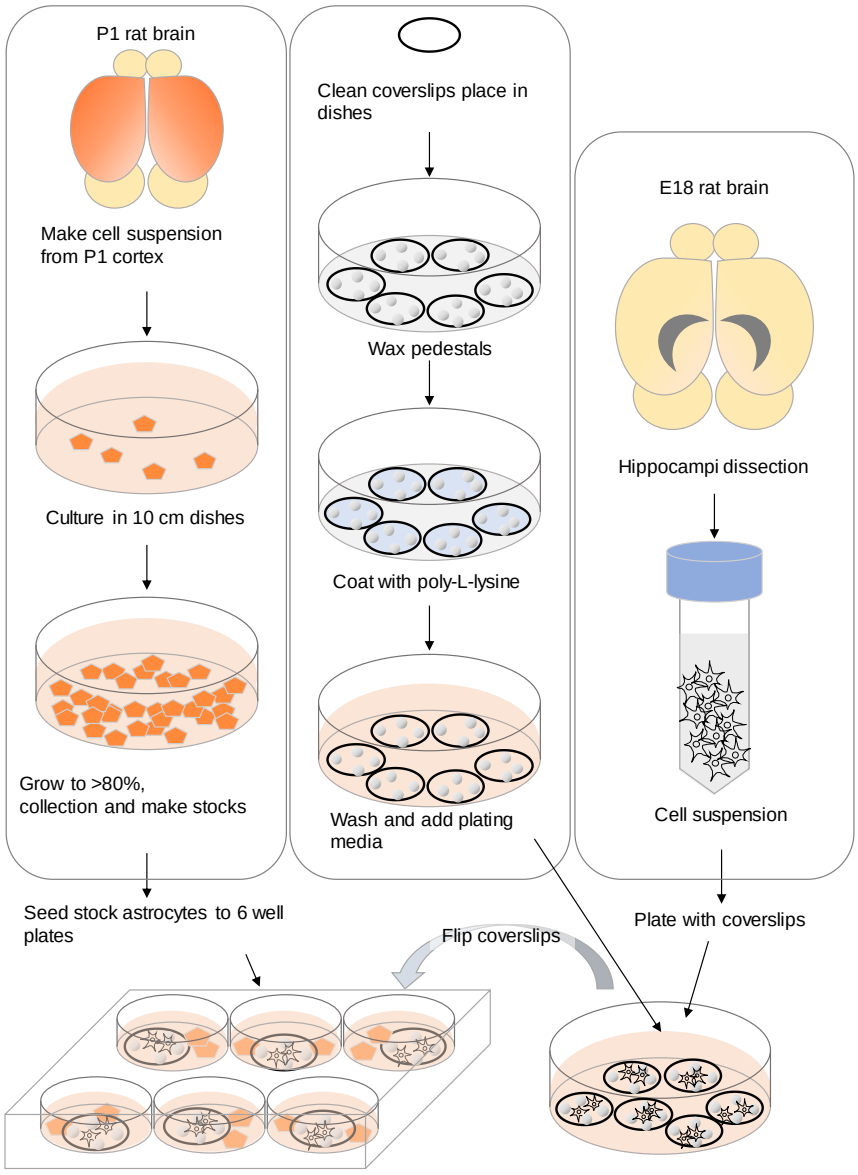

Fig. 8. **Primary astrocytes and neurons culture system**

Preparation of astrocytes, coverslips, and primary hippocampal neurons. Astrocytes are collected from P1 rat brain cortices and cultured. They are stored as frozen stocks. They are thawed and cultured before preparing hippocampal culture. Clean coverslips are decorated with paraffin and coated with poly-L-lysine. Hippocampal neurons are collected from E18 rat brains and plated on the coverslips. Once they attached to the coverslips, they are transferred to the plates with astrocytes.

2.1.1. Primary astrocyte culture system

Astrocytes were prepared from cortices of postnatal SD rats (P0 or P1). Cortical neurons were dissociated in 0.25% trypsin/EDTA in DPBS without Ca^{2+} and Mg^{2+} and plated at 3×10^5 cells on poly-L-lysine (25 μg/ml) (**Table 1**) coated 10 cm culture dishes (Nunc # 150466) in Glial Plating Media (GPM, **Table 2**). Next day, the media were changed with fresh GPM. After that, medium change was done every 3 days. Astrocytes were collected when its density exceeded about 80%. They were washed with Dulbecco's PBS without Ca^{2+} and Mg^{2+}, incubated in 0.05% trypsin/EDTA at 37℃ for 5-10 min. They were collected in GPM and centrifuged at 1,000 rpm for 5 min. After removing the supernatant, cells were resuspended in GPM and aliquoted in cryotubes. They were supplemented with 10% DMSO and put in a -80℃ freezer in a cell freezing container. A few days later, these cryotubes were transferred to liquid nitrogen.

Table 1 **Poly-L-lysine solution**

1 mg/ml Poly L Lysine (P2636-1G, Sigma)
Dissolve 100 mg in 100 ml 0.1 M Borate Buffer (pH 8.5)
Make 50 ml aliquots and keep in -20 ℃
0.1 M Boric Acid
Dissolve 3.09 g in 500 ml sterile water
Adjust pH to 5.6
0.1 M Sodium Brate
Dissolve 19.068 g in 500 ml sterile water
Adjust pH to 8.67
Borate Buffer
500 ml 0.1 M Boric Acid
450 ml 0.1 M Sodium Borate
Adjust pH to 8.5

Recipe of poly-L-lysine solution. This solution was used to coat culture plates and coverslips.

2.1.2. Preparation of astrocyte culture for neuronal culture

Astrocytes were thawed and plated at 3×10^4 cells per well on poly-L-lysine (25 μg/ml) coated 6

well plates in GPM (3 ml/well). Media were changed next day and every 2-3 days afterward. GPM in astrocytes culture was changed to 5 ml of Neuronal Maintenance Medium (NMM, **Table 2**) at the day before dissecting hippocampi (see below). NMM was prepared by adding each solution shown in **Table 3**.

Table 2 **Culture Media**

Glial Plating media (GPM)
To 500 ml MEM (nacalai tesque)
Add 50 ml Horse Serum
10 ml of 30 % Glucose
5 ml Penicillin-Streptomycin Mixed Solution
Neuronal Maintenance Media (NMM)
To 500 ml MEM (nacalai tesque)
Add 5 ml Penicillin-Streptomycin Mixed Solution
2.5 ml of 1 mg/ml Insulin
5 ml of 10 mg/ml Apo transferrin
5 ml of 100 mM Na pyruvate
50 µl of 200 µM progesterone
50 µl of 300 µM SeO_2
2.5 ml of 20 mM Putrescine
10 ml of 30 % Glucose
5 ml of B27 (invitrogen)

2.1.3. Preparation of coverslips

Round coverslips (25 mm diameter) were placed in porcelain racks and soaked in 1 N nitric acid overnight. They were washed with milliQ water three times for 30 min each on a shaker. Washed coverslips were autoclaved and dried in a biosafety cabinet overnight. Dried coverslips were placed in 10 cm dishes (6 coverslips per dish) and added paraffin wax as dots near the edge. These paraffin dots served as pedestals when the coverslips with neurons were put into the 6-well plates with astrocytes with the neuronal side facing down. Paraffin dots were dried overnight (see **Fig. 6**). Coverslips were covered with 1 mg/ml poly-L-lysine (0.5 ml) and kept in a CO_2 incubated until the day of hippocampal dissection. Coated coverslips were washed with autoclaved water twice and

deionized, sterilized water (nacalai tesque #06442-95) once and covered with 10 ml of GPM before plating neurons.

Table 3 **Stock solutions for NMM**

1 mg/ml Insulin (Sigma I5500)
Dissolve 100 mg in 100 ml 0.01 M HCL
Make 2.5 ml aliquots and keep in -20 ℃
10 mg/ml Apo transferrin(Sigma T2252)
Dissolve 500 mg in 50 ml sterile water
Make 5 ml aliquots and keep in -20 ℃
100 mM Na pyruvate (Gibco)
Keep in 4 ℃
20 mM Putrescine (Sigma P7505)
Dissolve 0.1611 mg in 50 ml sterile water
Make 2.5 ml aliquots and keep in -20 ℃
200 μM progesterone (Sigma P0130)
Dissolve 6.3 mg in 1 ml ethanol and dilute 100 × in sterile water
Make 1 ml aliquots and keep in -20 ℃
300 μM SeO_2 (Sigma 200107)
Dissolve 1.65 mg in 50 ml sterile water
Make 1 ml aliquots and keep in -20 ℃
30 % Glucose (nacalai tesque)
Dissolve 150 mg in 500 ml heated sterile water
Run through filterd bottle in clean bench and keep 4 ℃
Penicillin-Streptomycine Mixed Solution (nacalai tesque)
Make 5 ml aliquots and keep in -20 ℃

2.1.4 Preparation of hippocampal neurons

Hippocampal neurons were prepared from timed-pregnant rats (E17 or E18). Rats were euthanized in a CO_2 chamber. The uterus was isolated from the mother, and rat embryos were collected from it. Heads of the pups were collected in a 60 mm dish containing DPBS without Ca^{2+} and Mg^{2+}. Brains were removed from the heads and placed in a 60 mm dish containing DPBS.

Embryonic hippocampi were dissected out and kept in DPBS on ice until finishing the dissection.

All hippocampi were transferred to a 15 ml conical tube and incubated with 5 ml of 0.25% trypsin/EDTA in DPBS for 15 minutes at 37 ℃ (every 5 minutes, the tube was gently inverted to mix). The trypsinization was ceased by adding 5 ml GPM, and the tissues were centrifuged at 1,000 rpm for 5 minutes. Supernatant was carefully removed using pipette. These trypsinized hippocampi were resuspended in 1 ml GPM using a 1 ml pipetman to dissociate cells. These cells were counted and plated at 5,000 to 50,000 cells per coverslip depending on experiments. Plated neurons were incubated in a 5% CO_2 incubator for 2 – 4 h, and the coverslips were transferred to the 6 well plates with astrocytes with the side with neurons facing down. At the second day, cytosine arabinofuranoside was added to the media at 5 μM (15.6 μl of 1.6 mM Ara-C). Half of the culture media was exchanged with fresh NMM at the seventh day in vitro (DIV).

2.2. DNA constructs

Human tau cDNA corresponding to the 0N4R variant (1 - 363 amino acid residues, see **Fig. 5**) was amplified and cloned into pRK172 using NdeI and EcoRI sites. For the deletion mutants, PRR2 and MTBD, corresponding regions (140 - 185 amino acid residues for PRR2 and 186 - 309 for MTBD) were removed using QuickChange mutagenesis. The coding regions of tau wild-type and mutants were amplified using PCR and cloned into pAcGFP (Clontech). Synthesized phospho-mimetic and dephospho-mimetic fragments (eurofins Genomics) were introduced into SacII and PstI site of pAcGFP-Tau. Resultant AcGFP-tau and mutants (GFP-tau hereafter) was then amplified using PCR and cloned into pLVSIN lentiviral vector (Clontech), of which CMV promoter was replaced with the TRE3GS element/promoter from pTetONE (Clontech).

2.3. Lentivirus preparation

HEK Lenti-X 293T cells were maintained in Dulbecco's Modified Eagle Medium (DMEM from Nacalai Tesque #08458-45) with 10% Fetal Bovine Serum (FBS from SIGMA) and 1 μg/ml penicillin and streptomycin in a 5% CO_2 incubator. For lentivirus preparation, trypsinized and

resuspended cells were plated at 1×10^6 cells per 10 cm culture dish a day before transfection. Plasmids for lentiviral components were used at 6 μg each of Rev, 2G, g/p (obtained from Addgene) with a plasmid for the gene of interest at 12 μg. Plasmids were mixed together and mixed with 50 μl of 2.5 M $CaCl_2$ and sterilized water to adjust to 500 μl.

Mixed plasmids solution was mixed with 500 μl of 2 times concentrated BES-buffered saline (BBS) and incubated at room temperature for 20 min. After the incubation, the mixture was dropped onto cells, and cells were incubated in a 3% CO_2 incubator. Next day (after about 16-20 h), medium was removed and replaced with 10 ml of NMM. Culture dishes were transferred to a 5% CO_2 incubator and incubated for 2 days. Culture medium was collected and transferred to a 15 or 50 ml conical tube through a 0.45 μm filter unit. Collected lentivirus was kept at 4℃ for short-term preservation or aliquoted for long-term preservation at – 80℃. For lentivirus titer measurement, p24 lentivirus titer kit (TaKaRa) was used. This kit measures the capsid protein in lentivirus using sandwich ELISA. The p24 protein of lentivirus in the sample was extracted in the Lysis buffer and bound to coated p24 antibody on a 96 well plate. Another anti-p24 antibody decorates the antigens, which are then detected with biotinylated second antibody, streptavidin-HRP and substrate solution (coloring reagent). The titer was calculated from the p24 level, and 10 multiplicity of infection (MOI) was used for experiments.

Cultured neurons were infected with lentivirus in 1~1.5 ml astrocyte conditioned NMM overnight 2~4 h after plating. After removing lentivirus, the expression of the gene of interest was induced with 1 μg/ml doxycycline in 1.5 ml astrocyte conditioned NMM for 1 h. Neurons were transferred back to the original 6 well plates with astrocytes.

2.4. Immunofluorescence

Neurons were fixed in 4 % paraformaldehyde/PBS for 20 min. Blocking and permeabilization was done in 4% dried milk/0.1 % Triton X-100/TRIS-buffered saline (TBS). Primary and secondary antibodies were diluted in the same buffer and applied in separate incubation steps of 1 h and 45

min, respectively. Coverslips were mounted on glass microscope slides using ProLong Gold anti-fade reagent (Thermo Fischer Scientific). We used the following primary antibodies (**Table 4**): rabbit anti-total tau (tauN) raised against the N-term peptide (AEPRQEFEVMEDHAGGGC) of human tau, rabbit anti-rodent tau (rodent tauN) raised against the peptide (DTMEDHAGDYTLLQDEG) corresponding to the N-terminal potion of mouse tau (serum at 1:1,000), rat anti-total tau (RTM38, serum at 1:5,000) raised against purified recombinant human tau (Kubo et al., 2019a), anti-human tau (tau12, mouse monoclonal antibody, 1:2000, Abcam), anti-GFP antibody (mouse monoclonal, 1:1,000, MBL), and chicken anti-MAP2 (serum at 1:2,000, Biosensis). Specificity and cross-reactivity of these antibodies to rodent and human tau have been validated (Kubo et al., 2019a).

Table 4 **Antibodies used in the study**

Antibody	**Immunogen**	**Dilution**	
RTM38	recombinant human tau	1:5000	From Dr. Miyasaka
Anti-tauN	Human tau peptide, AEPRQEFEVMEDHAGGGC	1:500000	From Dr. Miyasaka
Anti-Rordent tauN	Mouse tau peptide, DTMEDHAGDYTLLQDEG	1:50000	From Dr. Miyasaka
Anti-His-tag	6xHis-tagged protein	1:2000	MBL
Anti-FLAG-tag	Mouse tau peptide, DTMEDHAGDYTLLQDEG	1:100000	MBL
DM1A	alpha Tubulin.	1:1000	abcam
Anti-MAP2	MAP2	1:5000	biosenseis

2.5. Fluorescence recovery after photobleaching (FRAP)

For FRAP, a coverslip with neuron was set in a imaging chamber and was covered with warmed 1×HBSS to room temperature (~25℃). The confocal microscopy was performed on Olympus FV-1000 microscope or Carl Zeiss LSM 700 with 63× oil immersion lens at ×4 digital zoom. Photobleaching area was carried out using a 405 nm wavelength laser for 500 ms. Single scan images were obtained every 1 sec for 70 to 180 sec.

FRAP data were background subtracted, compensated for bleaching from the time-lapse imaging,

and normalized to make the minimum and maximum 0 and 1, respectively (Jensen et al., 2017). The recovery phase from the minimum was fitted with the one-phase association model: $Y= Y0 + (Plateau – Y0) \times (1 – 10^{-k \times X})$. The difference of the fitted curves among different tau variants, in different areas in neurons, or at different culture durations were analyzed with F-test for the null-hypothesis that a curve with shared parameters (slope k and Plateau) fits better than those with different parameters for each data set. We also fitted data from individual neurons and obtained averaged slope and Plateau for each mutant.

2.6. Imaging and localization analysis

To compare the localization of tau mutants relative to that of endogenous tau, we measured average fluorescence intensities of expressed tau in a dendrite and the axon and computed the ratio of axonal over dendritic signals. The value was normalized to that of endogenous tau in the same neuron. We obtained normalized ratios from 6~8 neurons for each tau mutant from at least two independent cultures. The averages were compared to that of WT tau using ANOVA with Dunnett's post hoc tests

.

3. RESULTS

3.1. Expressed tau mis-localizes in cultured neurons

The tau-1 antibody has been widely used to label the axons, as dephosphorylated tau at Ser195, Ser198, Ser199, and Ser202 (Szendrei et al., 1993) has been shown to highly accumulate in the axons of immature neurons in culture (Mandell and Banker, 1996). Although total tau has also been shown to be accumulated in distal axons (Mandell and Banker, 1996), its precise subcellular localization has not been extensively studied. Using antibodies recently developed (Kubo et al., 2019a), which can detect unaggregated tau at high sensitivity and independently of phosphorylation, I confirmed that total endogenous tau is highly accumulated in distal axons even in stage 3 neurons in 2 ~ 3 DIV cultures and fully localized to the axon at 7 DIV (see **Fig. 9**).

With the axonal localization of total tau confirmed, I next checked whether transfected tau localizes to the axon as previously reported from a number of groups, and if a new experimental model was truly necessary. Expression plasmid encoding wild-type (WT) human tau with four microtubule binding repeats (four repeat human tau) with a CMV promoter was used to transfect primary rat hippocampal neurons at 7 days in vitro (DIV). Transfected neurons were fixed at 9 DIV. Endogenous and exogenous tau were detected using anti-rodent tauN antibody, which detects rat tau but not human tau, and anti-His tag antibody, respectively. I found that substantial levels of human tau remained in the soma and dendrites, while a fraction of it distributed to the axon (see **Fig. 7**). In contrast, even in these relatively young neurons, endogenous tau was predominant in the axon with a minor somatodendritic distribution. These results demonstrate that exogenous tau expressed in this conventional way does not localize to the axon. In a previous study in the laboratory, it was shown that different splicing isoforms (three-repeat tau) or rodent tau instead of the four-repeat human tau exhibited similar somatodendritic distributions, indicating that the isoform is not the issue. Therefore, I decided to establish a method to achieve axon-specific localization of exogenous tau, which would allow me to elucidate axonal localization mechanisms of tau.

3.2. Developmental changes of tau localization

A previous study from the laboratory has recently showed that tau mRNA expression is high during the first week of postnatal development and dramatically reduced in adult in mice (Kubo et al., 2019b). The study also demonstrated that expressing human tau in the same manner as endogenous tau results in its axonal localization in knock-in mice, whereas human tau expressed beyond the developmental period mis-localizes to the soma and dendrites in tau transgenic mice (Kubo et al., 2019b). From these findings, I speculated that mimicking the expression profile of endogenous tau during development may make exogenous tau localize to the axon in cultured neurons as well.

To test this, it is necessary to know when the expression and localization occur during neuronal maturation in culture. Cultured neurons were fixed at different time points and immunostained for endogenous tau using RTM38 antibody and MAP2. As described in Introduction (**Fig. 4**), immediately after plating, neurons are round and have only lamellipodia (stage 1). They start to extend filopodia and form several neurites (stage 2). Then, one neurite extends quickly and becomes the axon (stage 3). This is known as polarization. These occur during the first few days (1~3 DIV) in culture. After that, the remaining neurites develop as dendrites (stage 4) during the first week (4~7 DIV) in culture. Neurons are considered mature, when dendrites develop dendritic spines, and when synapses are formed (at >14 DIV). **Fig. 9** shows the localization of endogenous tau (green) and endogenous MAP2 (red) at 1, 3 and 7 DIV. In stage 2 neurons at 1 DIV, tau and MAP2 distributed in the soma and neurites, although there were some differences in their localizations. In stage 3 neurons at 3 DIV, MAP2 localized mainly in the soma and dendrites and was scarce in the newly formed axon. In contrast, tau (green) was preferentially distributed to the axon even at this initial axon specification stage. In stage 4 neurons at 7 DIV, the segregation of MAP2 and tau into the somatodendritic and axonal compartments became substantially clearer.

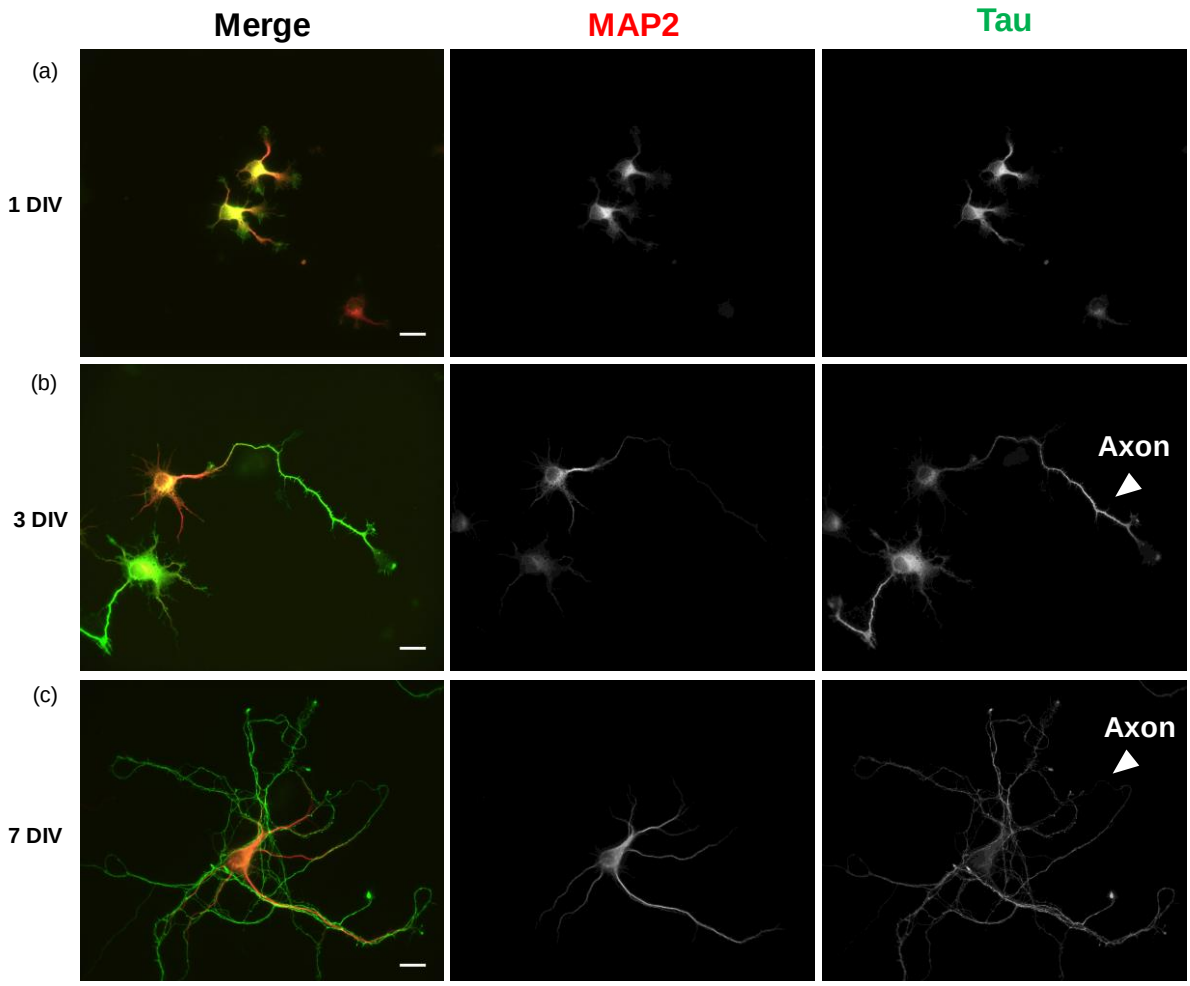

Fig. 9. **Developmental changes of tau localization**

Tau localization changes during neuronal development. Tau is shown in green. MAP2 is shown in red. Tau was detected at 1 DIV in stage 2 neurons (a). Tau was preferentially distributed to the axon at 3 DIV in stage 3 neurons (b). Axonal localization of tau was more refined at 7 DIV in stage 4 neurons (c). Arrow head is the axon (b, c). Scale bar: 20 μm.

In addition, I noticed that the fluorescence intensity of tau labeling appeared to be higher in stage 3 neurons than stage 4 neurons based on the immunofluorescence signals. This is consistent with the recent report that tau expression is at the highest during the first postnatal week in the mouse brain (Kubo et al., 2019b). Therefore, I hypothesized that tau is expressed transiently in early developmental stages and rapidly localizes to the axon in cultured neurons. Based on these results, I considered that exogenous tau needs to be expressed transiently in early developing neurons like endogenous tau to be localized to the axon.

3.3. Establishing an experimental model for studying tau localization

To mimic the early and transient expression of endogenous tau, it is necessary to be able to introduce the tau gene to very young neurons, which are not transfection-competent. Also, the expression needs to be controlled temporally. To achieve this, I sought establish a lentivirus expression vector combined with the tet-on system (**Fig. 10**). The tet-on system contains the tet-on regulator, which binds to a tetracycline response element (TRE) only in the presence of doxycycline and induces the target gene expression. Using the tet-on system enables tunable expression of tau. As I planned to test pathological mutants of tau found in FTDP-17 in future experiments, I chose to use four repeat human tau instead of rodent tau in my research. Cultured neurons were infected with lentivirus encoding wild-type four repeat human tau tagged with the His-tag at different multiplicity of infection (MOI) at 0 DIV (3~5 h after plating), and the expression was induced at different durations using doxycycline to find an optimal condition. I determined an optimal MOI for infectivity to neurons. I also found that 1 h induction is sufficient for detectable expression of human tau. This 1 h induction is used for the rest of the experiments.

To verify whether transient expression is what is necessary for the axonal localization of tau, I induced the expression at 7 DIV for 1 h and fixed at 14 DIV. MAP2, exogenous tau (anti-His-tag antibody), and endogenous tau (rodent tauN) were immunostained. Fluorescence intensity for each protein was measured in a dendrite and the axon. Exogenous human tau induced at 7 DIV was distributed throughout the cell in the axon as well as the soma and dendrites (**Fig. 11**). Line scan analysis of a region containing a dendrite and the axon revealed overlapping distribution of human tau and MAP2 as well as human tau and endogenous tau (**Fig. 11**). Therefore, I concluded that the transient expression itself was not sufficient to localize exogenous tau to the axon in stage 4 neurons.

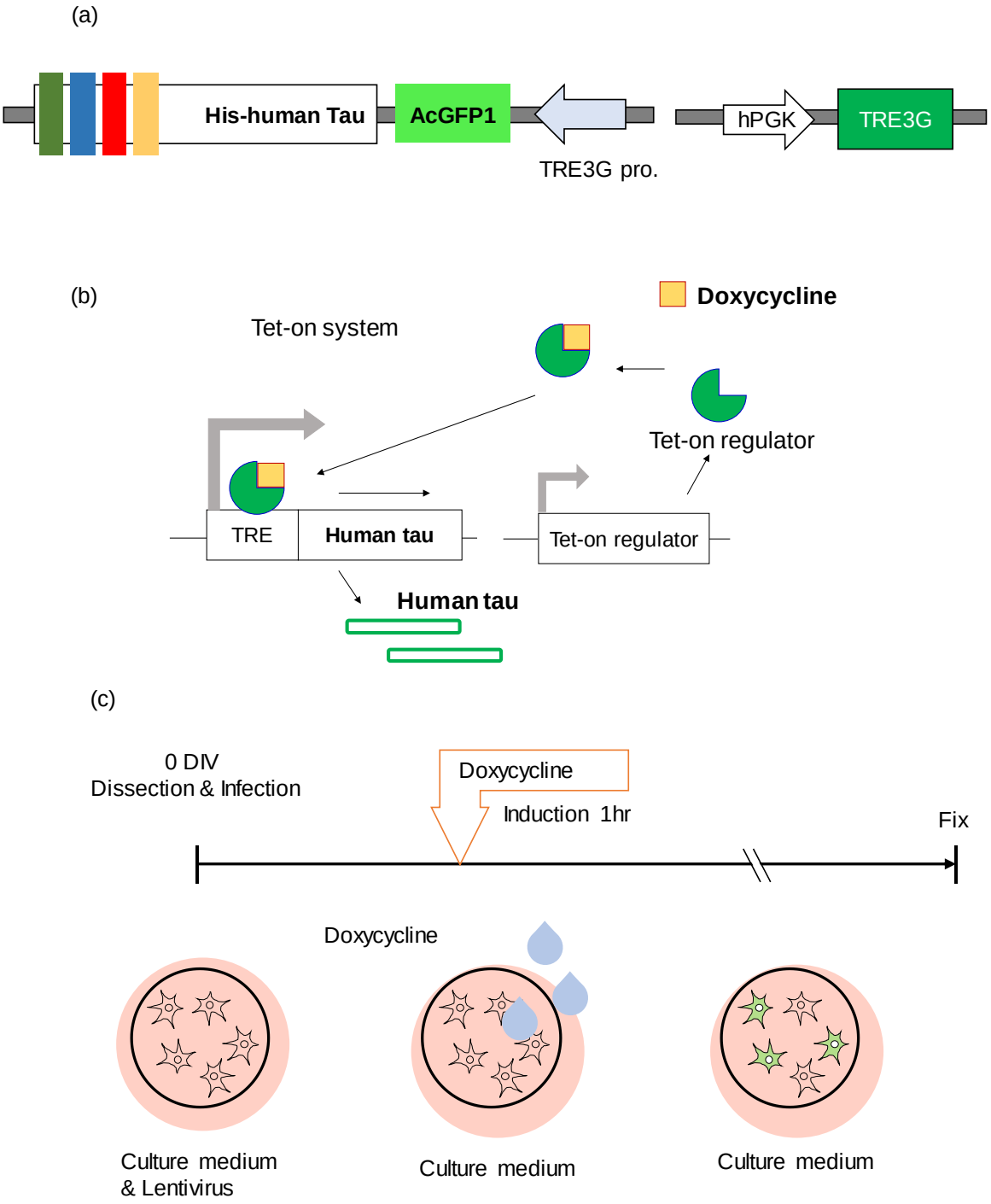

Fig. 10. **Inducible expression of tau using a tet-on system**.

Human tau with four MT-binding repeats (colored regions) with the His-tag and AcGFP was constructed into a lentiviral vector with the TRE3G promoter. TRE3G was also constructed into a lentiviral vector with a PGK promoter (a). Lentiviral particles were prepared separately. Co-infection of neurons with these viral particles enables inducible expression of human tau with doxycycline (b). Neurons were infected 3~5 h after plating. The expression was induced at 1 DIV for 1 h with doxycycline (c)

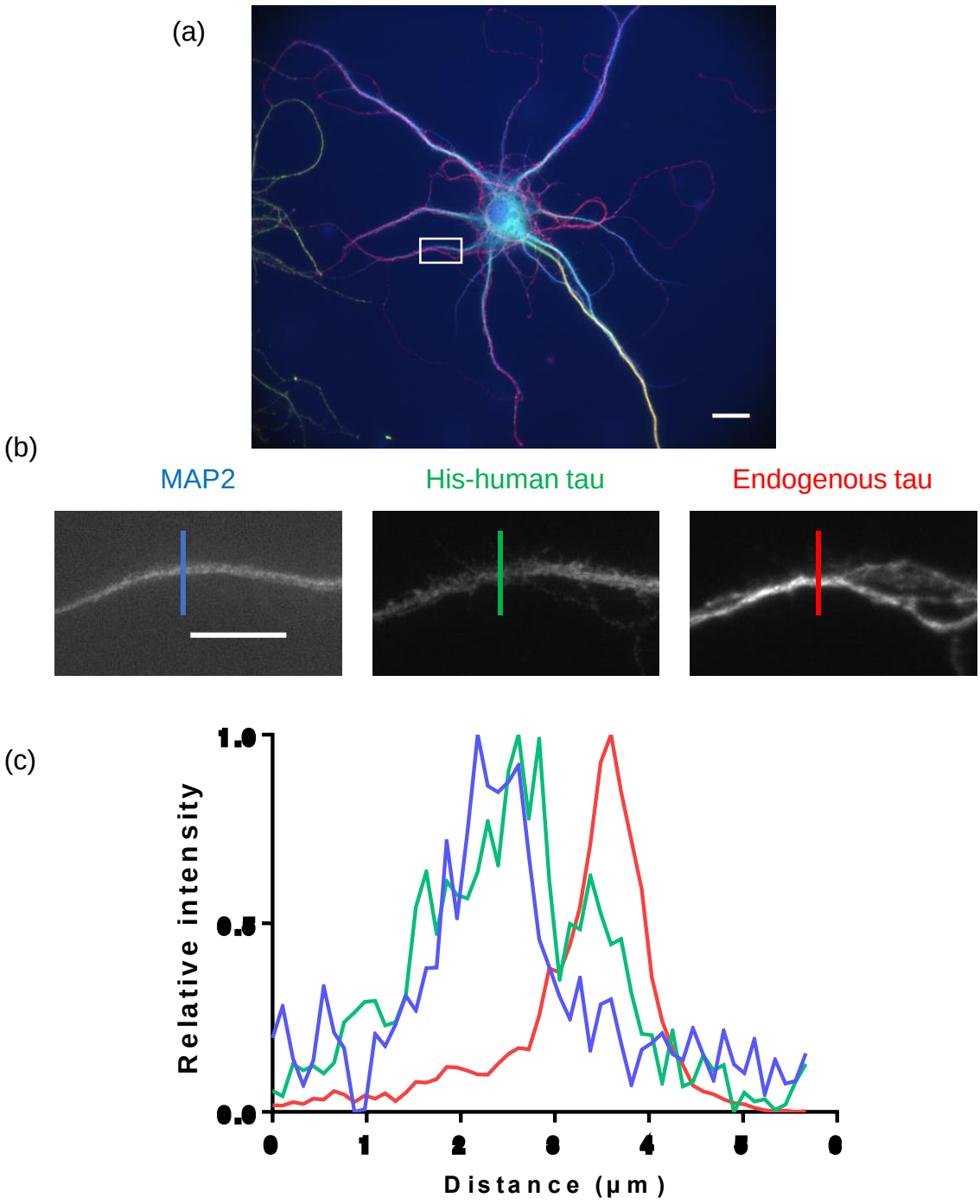

Fig. 11. **Mis-localization of exogenous tau**

The expression of human tau was induced for 1 h at 7 DIV. Neurons were fixed at 14 DIV and immunostained. Human tau (green) pre-dominantly distributed to the soma and dendrites with MAP2 (blue), whereas endogenous tau (red) was localized to the axon. Scale bar: 20 μm (a). High magnification images of the boxed area in (a) shows the dendritic distribution of human tau (b). In the line scan analysis of the images in (b), the intensity peak of exogenous tau overlaps with that of MAP2.

In contrast, when the expression was induced at 1 DIV for 1 h, the localization of human tau became very specific to the axon at 14 DIV (**Fig. 12**). Line scan analysis showed virtually complete overlap of human tau with endogenous tau and the absence of human tau from a MAP2-positive dendrite (Fig. 11). Both 3 and 4 repeat tau exhibited similar results (data not shown).

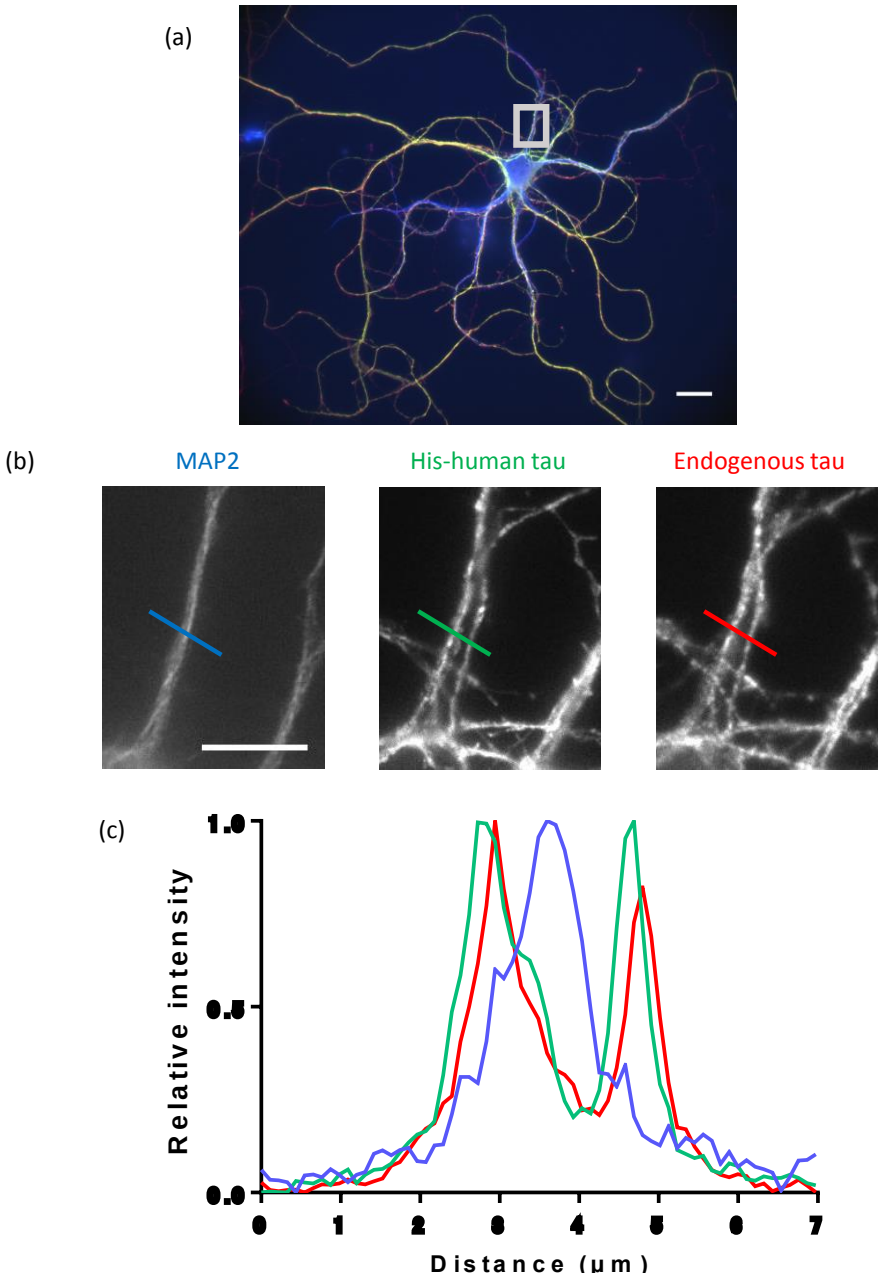

Fig. 12. **Temporary expression of human tau in immature neurons results in its axonal localization** The expression of human tau was induced for 1 h at 1 DIV. Neurons were fixed at 14 DIV and immunostained. Human tau (green) was localized to the axon with endogenous tau (red) and largely absent from dendrites positive for MAP2 (blue). Scale bar: 20 μm (a). High magnification images of the boxed area in (a) shows the co-localization of exogenous tau with endogenous tau in the axon (b). In the line scan analysis of the images in (b), the intensity peak of exogenous tau overlaps with that of endogenous tau but not MAP2.

These results indicate that transient expression in immature neurons is critical to localize exogenous human tau to the axon like endogenous tau. However, it is still possible that human tau expressed in mature neurons may just need more time to be fully axonal. To know this, neurons were incubated with doxycycline at 7 DIV for 1 h and fixed at 24 DIV instead of 14 DIV. I found that some neurons exhibited more axonal localizations but still with overlapping signals with MAP2 signals **(Fig. 13**). But many others showed human tau remaining in the soma and dendrites as shown in **Fig. 14**. These results indicate that tau expressed beyond the early developmental stages is strongly retained in the soma and dendrites, even when the expression is made transient. These results suggest that the timing and pattern of expression is critical for the axonal localization of human tau as observed in the mouse brain in previous studies from the laboratory (Kubo et al., 2019b).

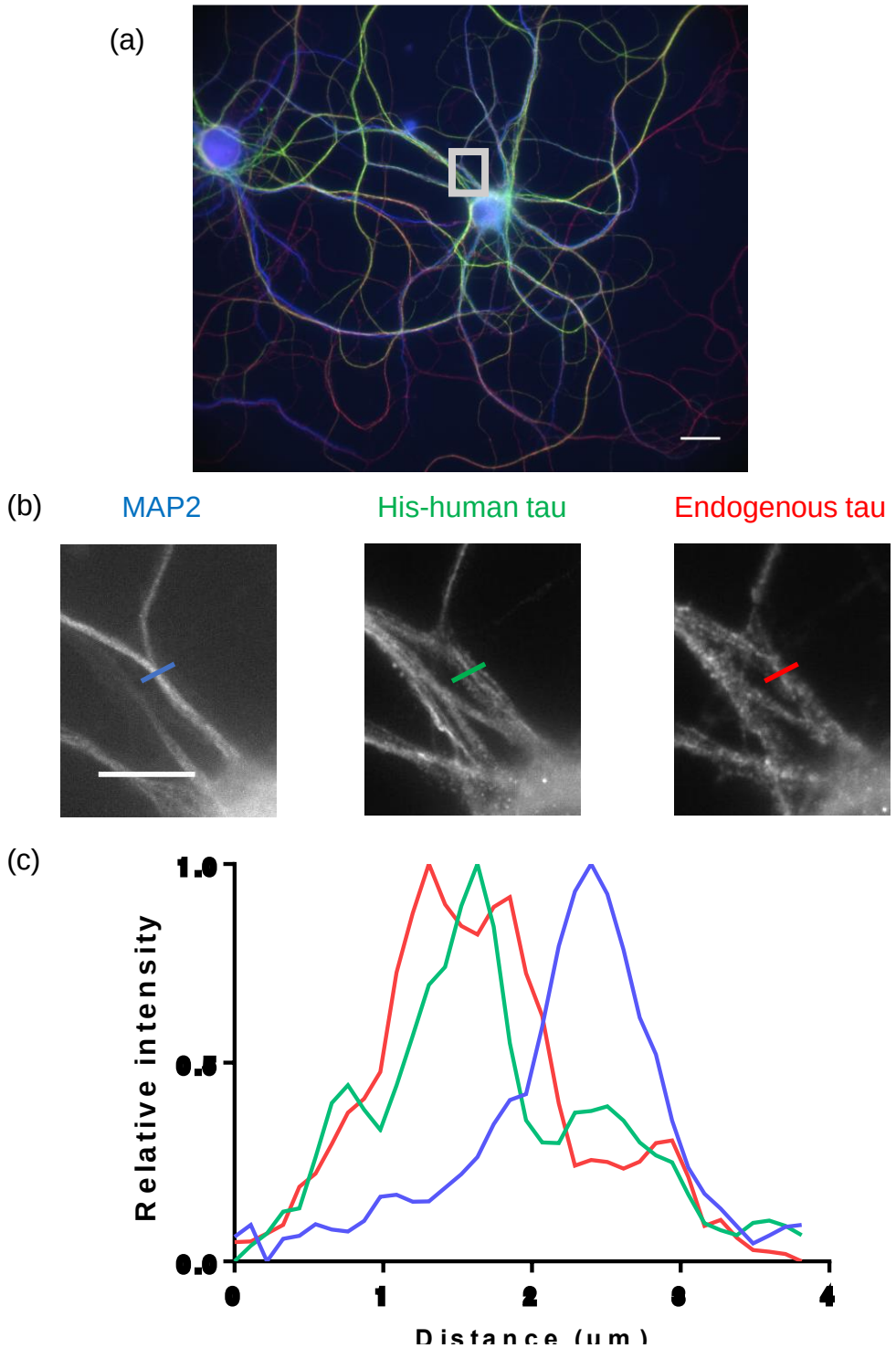

Fig. 13. **Sustained axonal localization of exogenous tau transiently expressed in immature neurons**

The expression of human tau was induced for 1 h at 7 DIV. Neurons were fixed at 24 DIV and immunostained. Human tau (green) was localized to the axon with endogenous tau (red) but still present in dendrites positive for MAP2 (blue). Scale bar: 20 μm (a). High magnification images of the boxed area in (a) shows the co-localization of exogenous tau with endogenous tau in the axon (b). In the line scan analysis of the images in (b), the intensity peak of exogenous tau overlaps with that of endogenous tau with some remaining signals in the MAP2-positive dendrites.

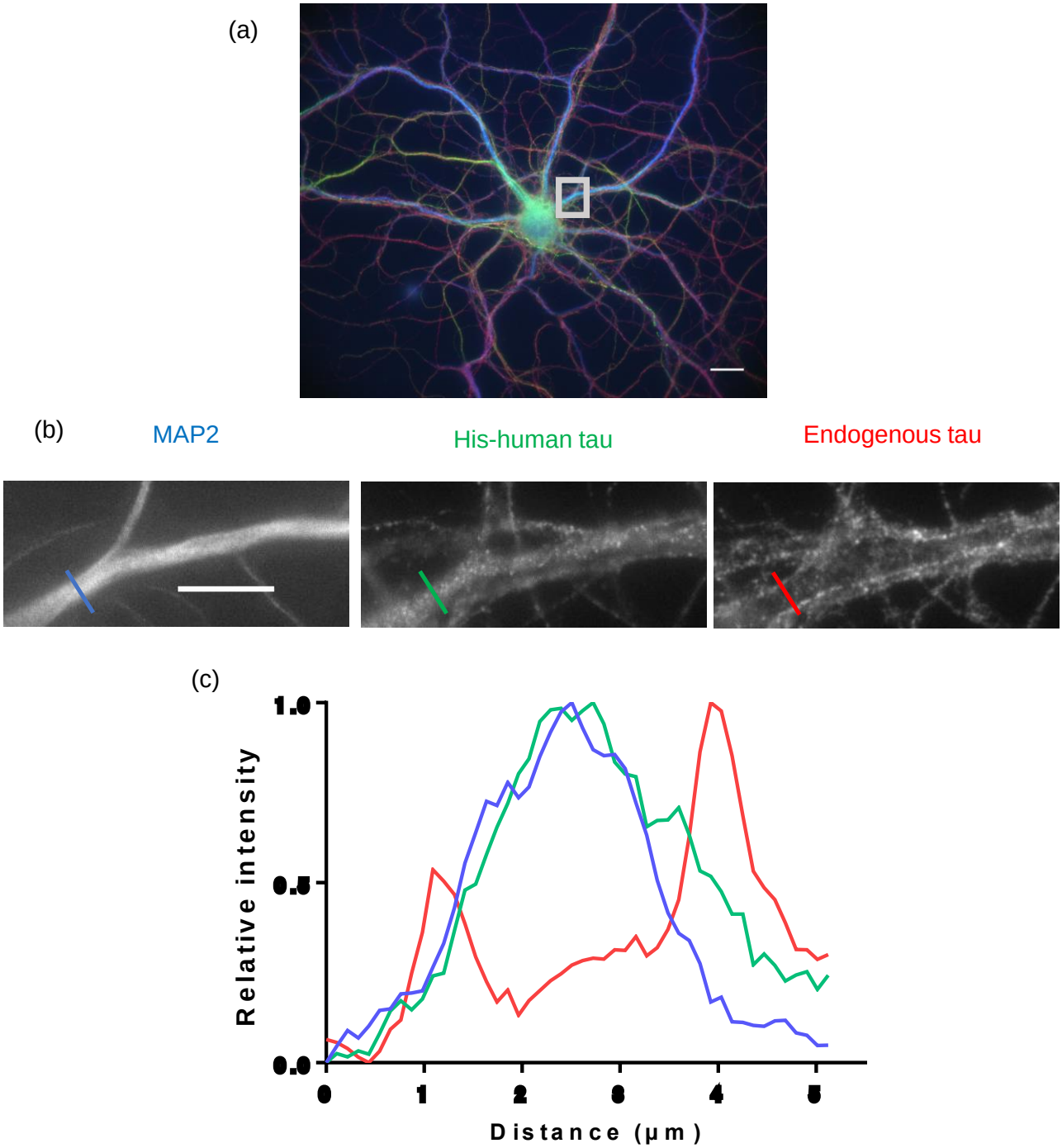

Fig. 14. **Sustained somatodendritic distribution of exogenous tau transiently expressed in stage 4 neurons**

The expression of human tau was induced for 1 h at 7 DIV. Neurons were fixed at 24 DIV and immunostained. Human tau (green) predominantly distributed to the soma and dendrites with MAP2 (blue), whereas endogenous tau (red) was localized to the axon. Scale bar: 20 μm (a). High magnification images of the boxed area in (a) shows the dendritic localization of exogenous tau (b). In the line scan analysis of the images in (b), the intensity peak of human tau overlaps with that of MAP2 but not endogenous tau.

Furthermore, exogenous human expressed tau early and transiently with my method distributed to the axon even in stage 3 neurons and colocalize with endogenous tau at 3 DIV (**Fig. 15**). This is the first demonstration of such axon-preferential distribution of human tau in immature neurons in culture. I considered this to be quite useful because it is difficult to identify the axon of an infected neuron in more mature cultures, due to its extended length and overlaps with the axons of other neurons. Using these stage 3 neurons seemed to make it easier to identify the axon and study how exogenous tau start to localize to the axon in early developmental stages. Therefore, I mostly focused on these stage 3 neurons to identify the determinants of the axonal localization of tau in the following experiments.

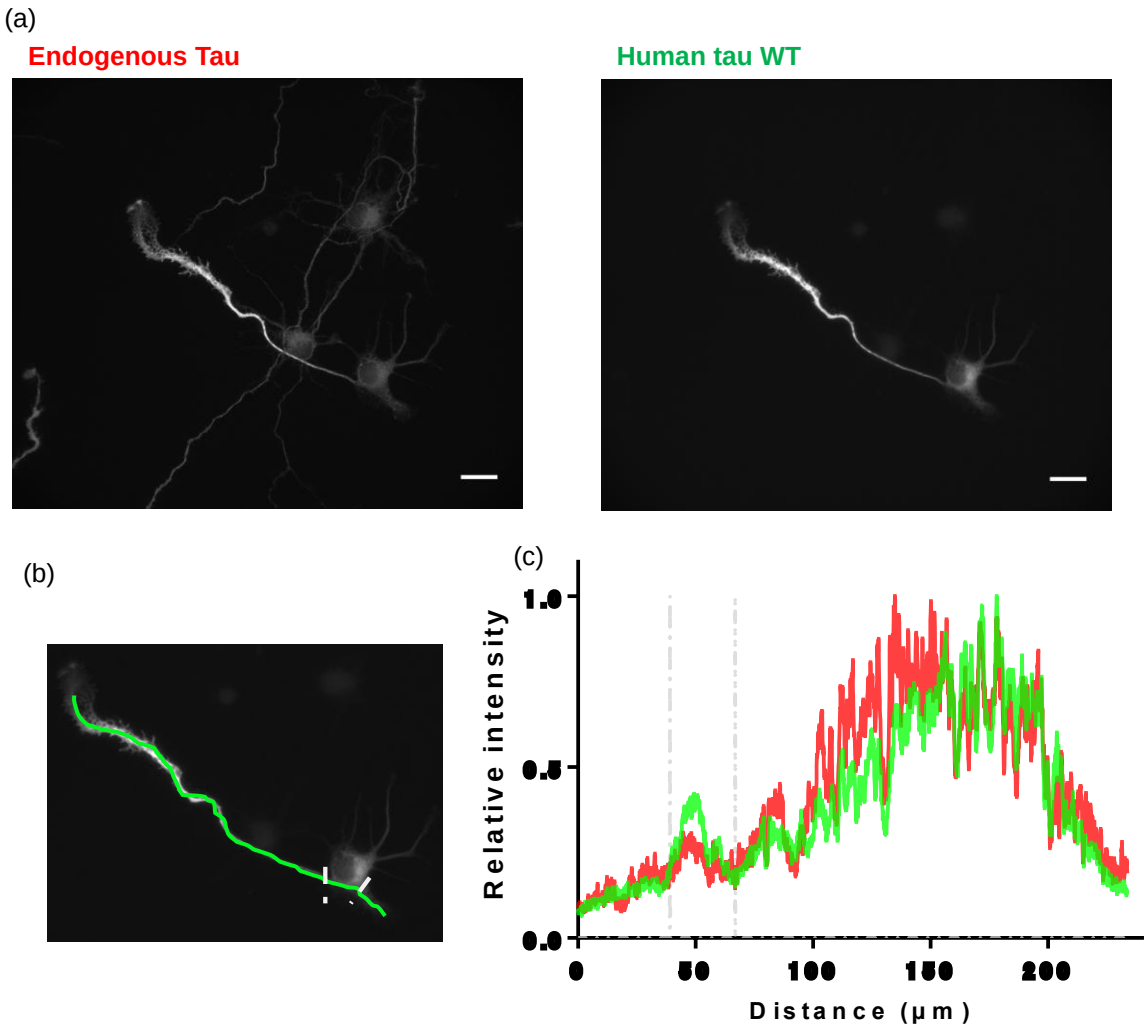

Fig. 15. **Reproduction of the early axonal localization with human tau**

With the transient expression at 1 DIV, exogenous tau (Anti-FLAG-tag, green) behaved like endogenous tau (Anti-rodent tauN, red) and localized to the newly formed axon in stage 3 neurons at 3 DIV. Scale bars: 20 µm. Line scan analysis of human tau and endogenous tau from a neurite through the soma and to the distal tip of the axon (b). The intensity peak of exogenous tau overlaps with that of endogenous tau (c). The vertical dotted lines indicate the borders between the neurite and the soma

3.4. Search for the determinants of the axonal localization of tau

To investigate which region of the tau protein is important for the axonal localization, I generated 9 deletion mutants of human tau. Nine regions were identified based on the amino acid sequence and known functional domains (**Fig. 16**) and deleted individually.

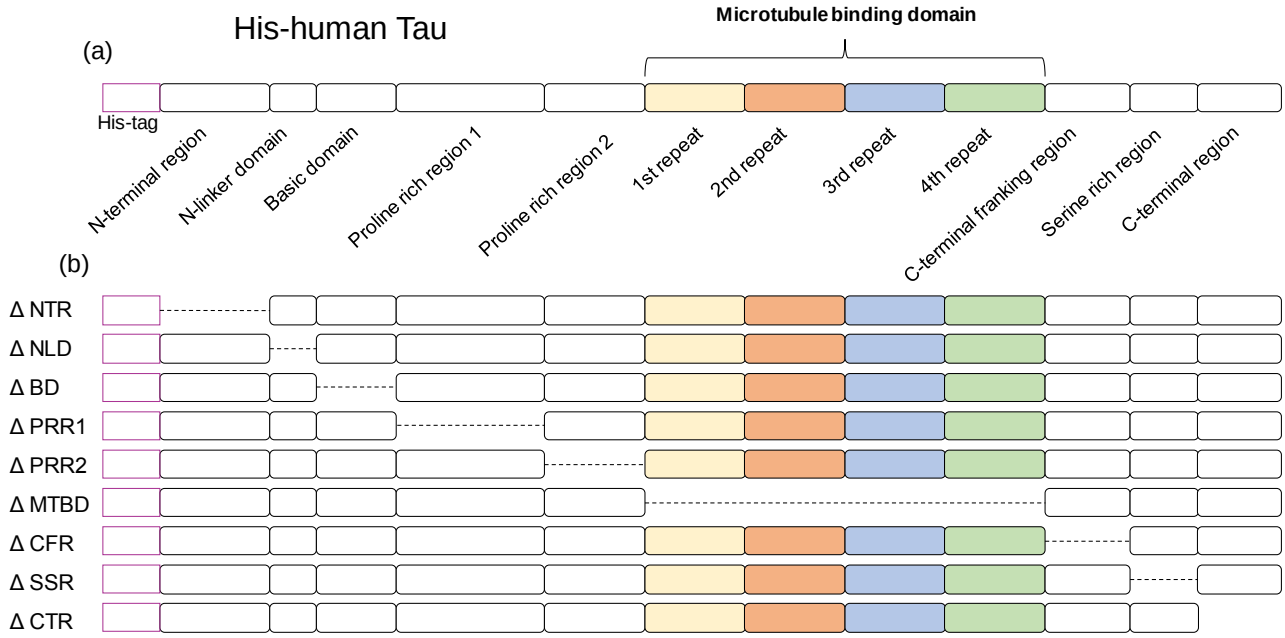

Fig. 16. **Schematic diagram of tau protein structure**

Tau primary structure is separated into 9 regions based on the primary structure and known functions (a). The schematic diagram of the deletion mutant (b). These mutants were named on the basis of each deletion region. (NTR:N-terminal region, NLD:N-linker domain, BD:Basic domain, PRR1:Proline rich region 1, PRR2:Proline rich region 2, MTBD:Microtubule binding domain, CFR:C-terminal franking region, SRR:Serine rich region, CTR:C-terminal region)

Each deletion mutant or WT tau was expressed in cultured neurons using my expression method. I fixed neurons at 2 or 3 DIV and compared the localizations of mutants and endogenous tau. To compare them quantitatively, I calculated the ratios of axonal signals over dendritic signals for endogenous and exogenous tau (WT and 9 mutant tau), and normalized the ratio of exogenous tau to that of endogenous tau in each neuron. Therefore, a colocalization of exogenous tau and endogenous tau would show a value close to one (**Fig. 17**). I found that removing the proline-rich region 2 (ΔPRR2) showed an abnormal distribution in the soma and dendrites, as well as in the axon (**Figs. 17 and 18**). As shown in **Fig. 17**, WT tau, which exhibits a similar enrichment in the axon to endogenous tau, had the ratio close to one. However, ΔPPR2 tau showed a significantly lower value, indicating that it is not enriched in the axon with endogenous tau. These results suggest that PRR2 is a critical region of tau for its axonal localization.

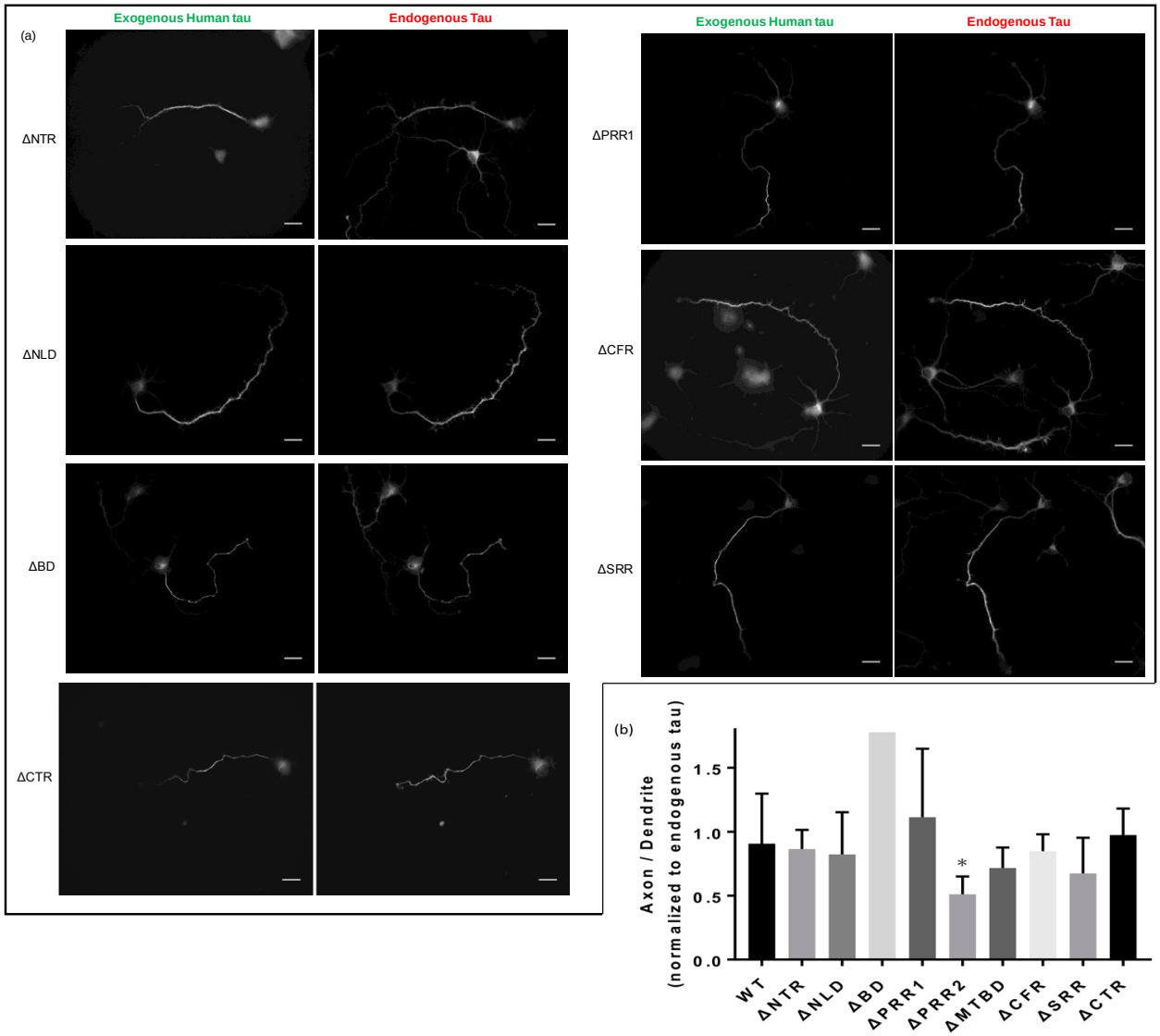

Fig. 17. **Quantitative analysis of localizations of the deletion mutants**

Neurons were infected with lentivirus encoding each mutant at 0 DIV, treated with doxycycline at 1 DIV for 1 h, fixed and immunostained for the mutant and endogenous tau at 3 DIV (a). Quantification of how exogenous tau is enriched in the axon using the ratio of axonal signals over dendritic signals normalized to that of endogenous tau. Colocalization of exogenous tau and endogenous tau would show a value close to 1 (b). WT : n=7 cells, ΔNTR : n=7, ΔNLD : n=12, ΔBD : n=1, ΔPRR1 : n=3, ΔPRR2 : n=9, ΔMTBD : n=7, ΔCFR : n=6, ΔSRR : n=6, ΔCTR : n=3. *p= 0.0345 using ANOVA with Dunnett's post hoc tests.

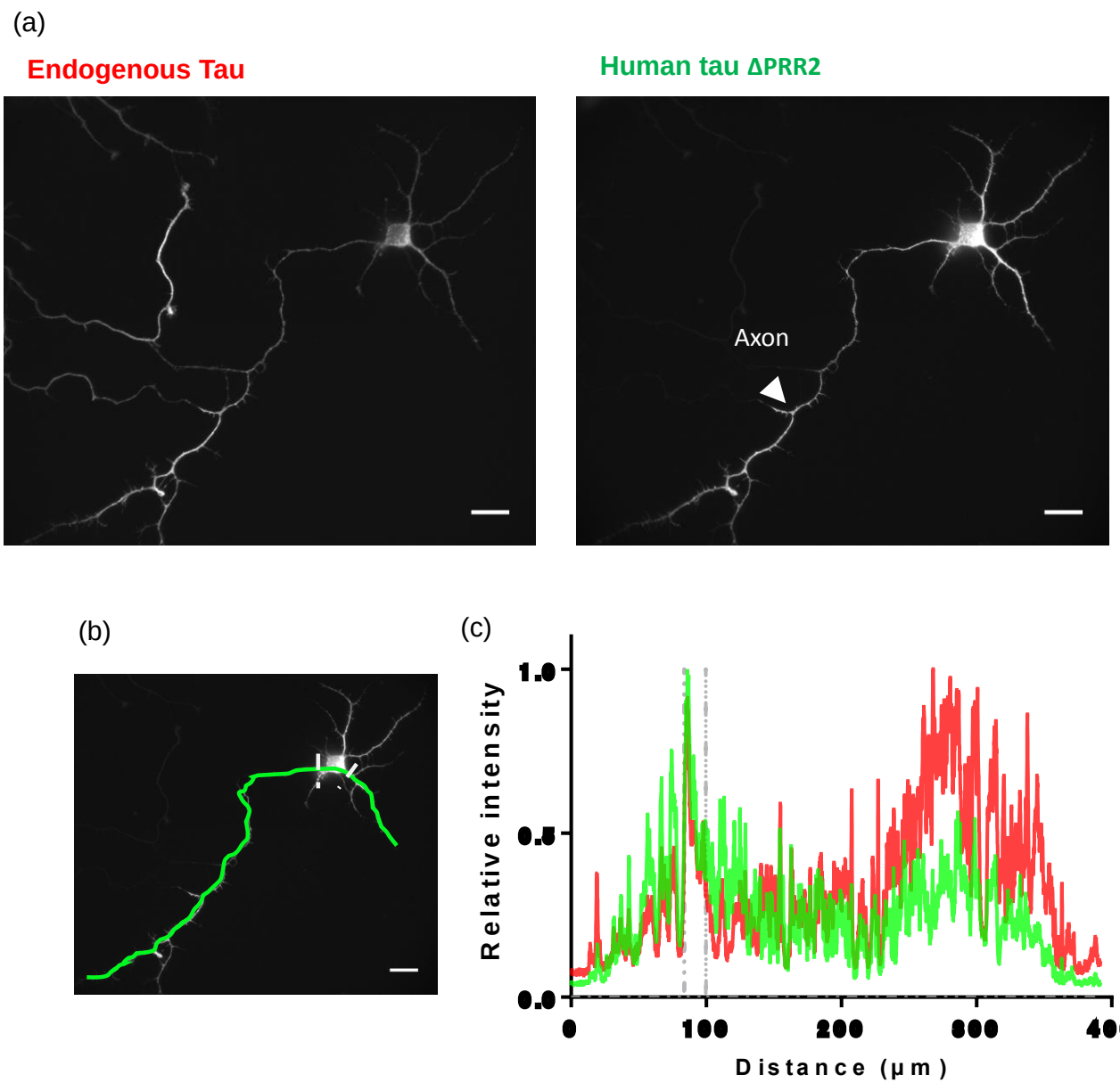

Fig. 18. **Localization of tau ΔPRR2 in stage 3 neurons at 3 DIV**

Neurons infected were fixed at 3 DIV and immunostained for endogenous tau (red) and ΔPRR2 (green). Signal intensities were adjusted to have similar intensities in the axon. Unlike WT (**Fig. 15**), ΔPRR2 was retained in the soma and dendrites. Scale bars: 20 μm. Line scan analysis of ΔPRR2 and endogenous tau from a neurite through the soma and to the distal tip of the axon (b). The intensity peak of ΔPRR2 appeared in the soma, instead of the distal axon with endogenous tau (c). The vertical dotted lines indicate the borders between the neurite and the soma and between the soma and the axon.

Tau is a MAP having a conserved MT-binding domain (MTBD). Previous studies have suggested that MTBD is important for the MT-binding and the axonal localization of tau (Kanai and Hirokawa, 1995; Utton et al., 2005; Falzone et al., 2009; Weissmann et al., 2009; Li et al., 2011; Scholz and Mandelkow, 2014). Therefore, I carefully analyzed tau mutant lacking MTBD (ΔMTBD). Surprisingly, ΔMTBD expressed using my system co-localized with endogenous tau in the axon at 3 DIV (**Fig. 19**). Quantitative analysis also suggested that ΔMTBD localized to the axon with endogenous tau like WT (**Fig. 16**). These results indicated that MTBD is not necessary for the axonal localization of tau.

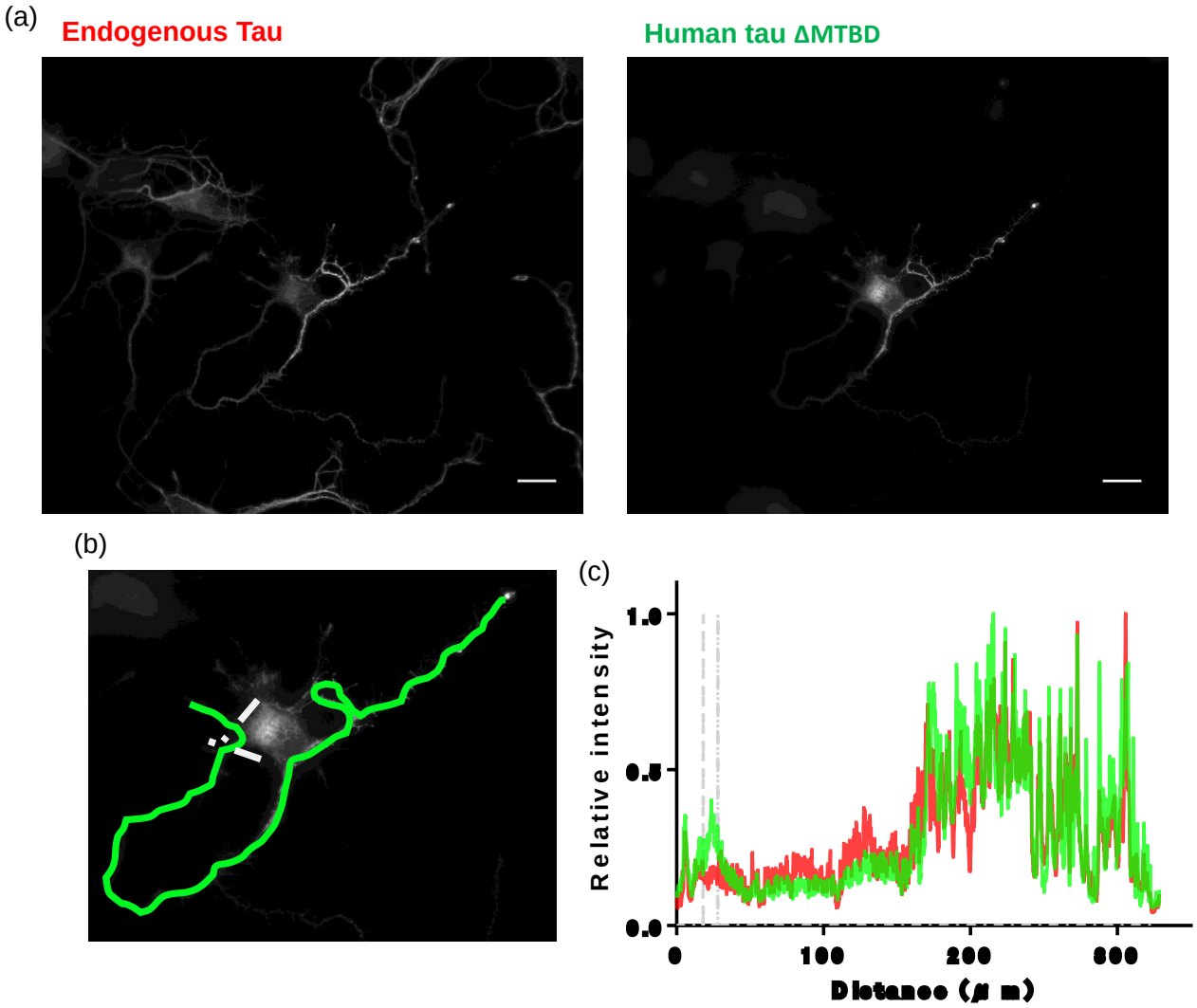

Fig. 19. **Localization of tau ΔMTBD in stage 3 neurons at 3 DIV**

Neurons infected were fixed at 3 DIV and immunostained for endogenous tau (red) and ΔMTBD (green). Signal intensities were adjusted to have similar intensities in the axon. Like WT (**Fig. 15**), ΔMTBD was localized to the axon (a). Scale bars: 20 µm. Line scan analysis of ΔMTBD tau and endogenous tau from a neurite through the soma and to the distal tip of the axon (b). The intensity peak of ΔMTBD appeared in the soma, instead of the distal axon with endogenous tau (c). The vertical dotted lines indicate the borders between the neurite and the soma and between the soma and the axon.

3.5. The mobility of tau revealed by live-cell imaging

The results of ΔMTBD were very surprising because it is not consistent with many of previous studies proposing the important roles of MTBD in tau transport and localization. Therefore, I examined whether ΔMTBD really lacks MT-binding and whether MT-binding is really unnecessary for the axonal localization in living neurons. To investigate MT-binding of tau in living neurons, I used the fluorescence recovery after photobleaching (FRAP) method. FRAP is a useful method to measure the mobility of molecules quantitatively by measuring the recovery of fluorescence after photobleaching induced by powerful laser. When the mobility of the fluorescent molecule is large, the recovery is fast. Also, the extent of recovery indicates how much portion of the molecules is mobile. When the recovery is fast and complete, it should be considered that the MT-bound tau is low, and when the recovery is slow and incomplete, it is considered that the MT-bound tau is high (**Fig. 20**). I thought that combining our expression method and FRAP would provide insight into how tau binds to MTs and is transported to the axon.

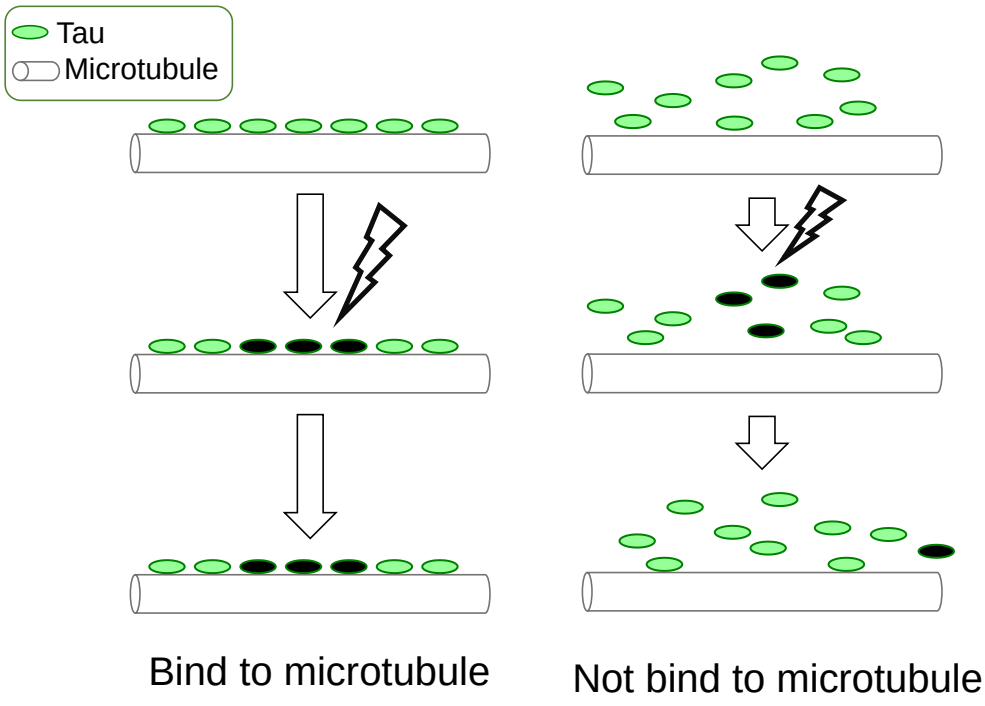

Fig. 20. **FRAP analysis of MT-binding of tau**
MT-binding of tau would affect the speed and the extent of fluorescence recovery.

Neurons expressing human tau tagged with AcGFP were mounted on an imaging chamber with Hank's balanced salt solution (HBSS, see Methods). I chose neurons with normal morphology and without too much overexpression. I estimated the expression of human tau to be comparable to that of endogenous tau, as the RTM38 antibody, which detect both human tau and rodent tau at similar sensitivity on Western blot (Kubo et al., 2019a), labeled expressing neurons with about two-fold fluorescence intensity compared to non-expressing neurons (data not shown). Laser was applied to a region of interest (3.5 μm diameter circle) for 500 ms after taking the pre-bleaching images for 10 frames. Images were taken every second. The fluorescence intensity in the bleached area was measured to calculate the recovery rate and mobile/immobile fractions using exponential growth functions.

Fig. 21 shows a 3 DIV neuron expressing AcGFP-tau. As shown in the direct fluorescence image, WT tau preferentially distributed to the newly formed axon. This verifies that the axonal localization detected using immunolabeling is not an artifact from epitope masking or preferential binding of the antibodies to axonal human tau. The mobility of human tau was measured in the axon. Its fluorescence recovered with a recovery rate of 0.075 ± 0.004 and an immobile fraction of 0.369 ± 0.023. Since neurons fixed with paraformaldehyde did not show any recovery, this result suggests that a significant fraction of tau is not bound to MTs and mobile. Also, the recovery was significantly slower than AcGFP alone, which is expected to be freely diffusible (data no shown).

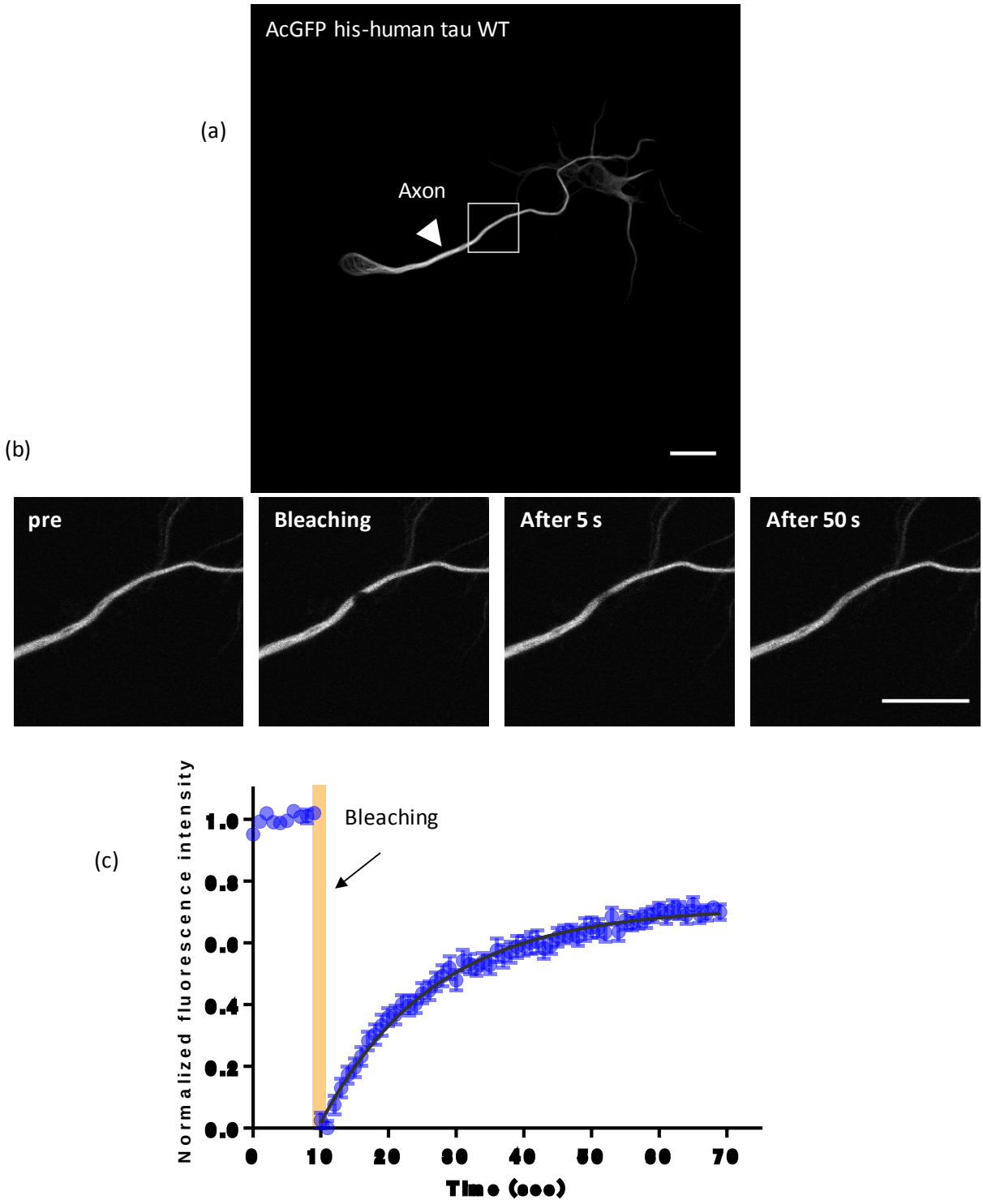

Fig.21. **FRAP of WT tau in stage 3 neurons at 3 DIV**

FRAP was performed on neurons, in which the expression of AcGFP-tagged human tau was induced for 1 h at 1 DIV, at 3 DIV. Direct fluorescence image is shown in (a). FRAP was performed in a middle portion of the axon. Images before, immediately after bleaching, and 5 s and 50 s after bleaching are shown (b). Recovery rate of fluorescence. The data shown are the mean ± SEM and fitted with an exponential growth function (c). Scale bars: 20 µm. Diffusion coefficient was showed in Table 5.

I then examined whether disruption of MTs changes the recovery rate and extent. If FRAP of tau really reflects its MT-binding in situ, the recovery rate and the extent of recovery would become similar to those of freely diffusion molecules after the disruption. Neurons were imaged before and after the treatment with nocodazole (1 μg/ml for 10~20 min). The recovery rate was greatly enhanced when MTs were disrupted with nocodazole (**Fig. 22**), suggesting that MT-binding of tau can be monitored with FRAP.

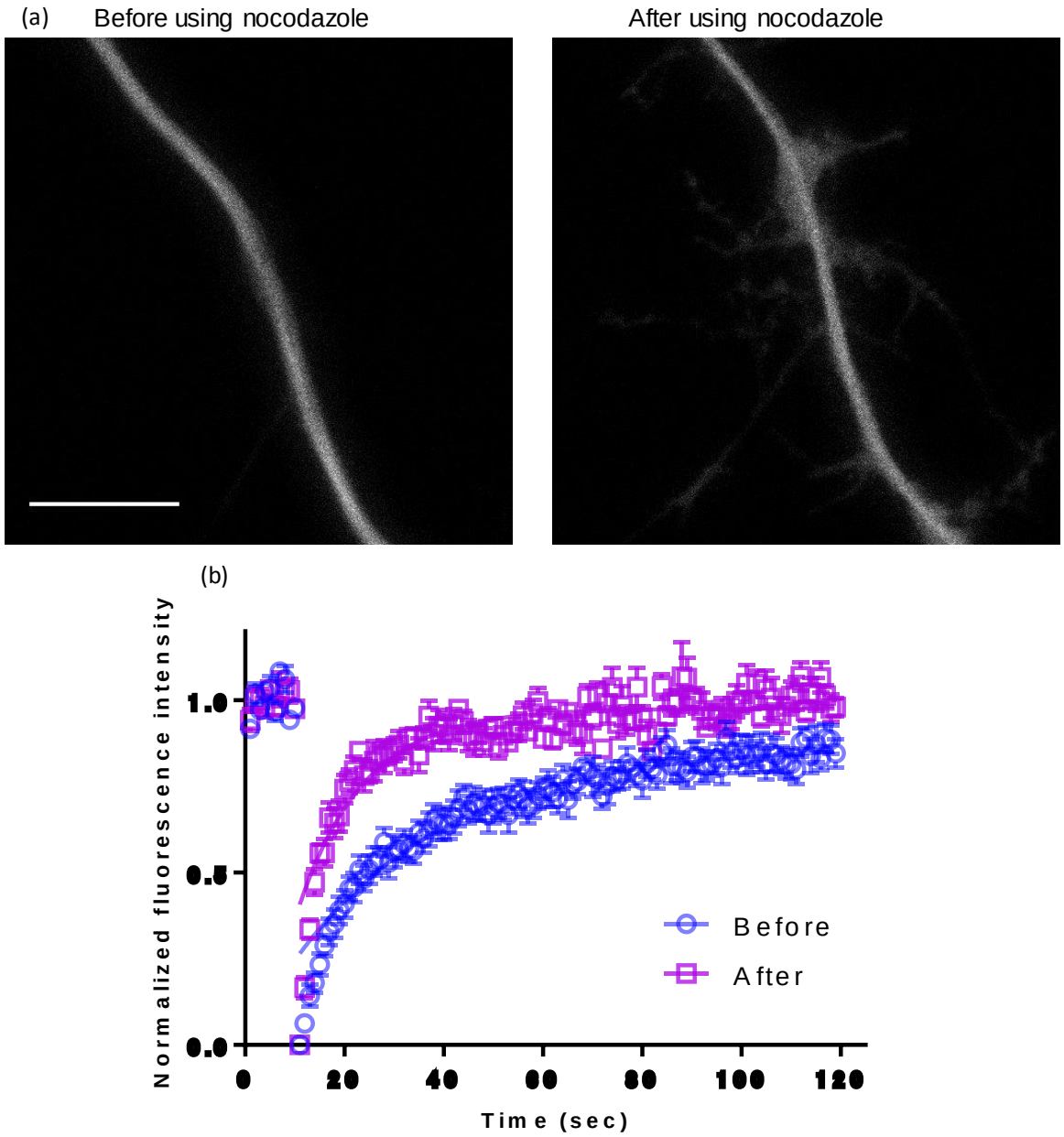

Fig. 22. **FRAP of WT tau after nocodazole treatment in stage 3 neurons at 3 DIV**
Nocodazole was used to induce MT depolymerization. Axons before and after the treatment (nocodazole 1 μg/ml for 10 min) (a). The recovery rates of fluorescence before and after the treatment were measured (b). The recovery rate and the extent increased in the axon after the treatment (n=4).

I also performed FRAP at different days in culture to examine whether MT-binding of tau changes during neuronal maturation. The mobility of WT tau did change during development. The mobility in the axon was decreased slightly but significantly between 3 and 14 DIV (**Fig. 23(a)**). In contrast, the mobility in the soma reduced dramatically between 7 and 14 DIV (**Fig. 23(b)**). These results suggest that binding to MTs of tau becomes more stable in the axon and particularly in the soma.

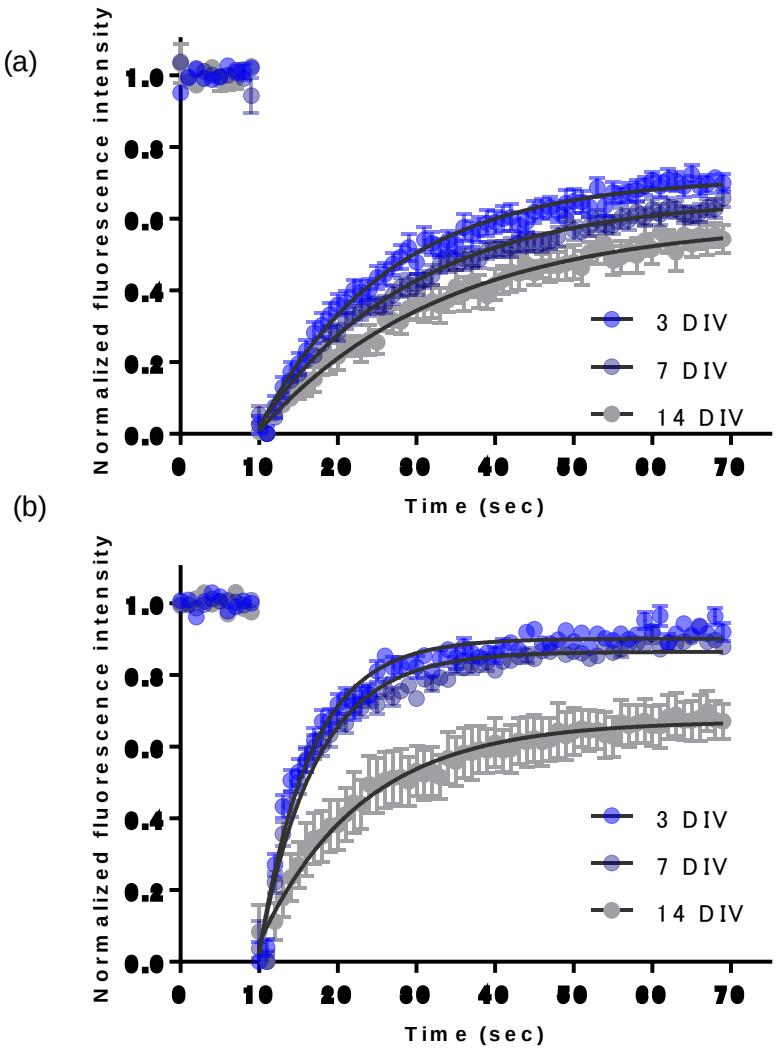

Fig. 23. **FRAP of WT tau at 3, 7, and 14 DIV**
Recovery rate of fluorescence in the axon (a) and in the soma (b) from neurons at 3, 7, and 14 DIV. The data shown are the mean ± S.E.M (3 DIV n=17, 7 DIV n=17, 14 DIV n=6 in the axon. 3 DIV n=12, 7 DIV n=12, 14 DIV n=6 in the soma).

From the deletion mutant experiments, I found that MTBD is not necessary for the axonal localization of tau. From these results, I assumed that ΔMTBD does not bind to MTs in neurons. Using FRAP, this can be tested in the soma, dendrites and the axons of living neurons. In fact, ΔMTBD showed significantly faster recovery than WT (**Fig. 24**). The recovery was also complete. This was quite similar to the results of AcGFP alone (data not shown). This high mobility of ΔMTBD therefore suggests that ΔMTBD does not stably bind to MTs in the axon. This is consistent with the reduced MT-binding of ΔMTBD in the in vitro binding assay (Iwata et al., 2019).

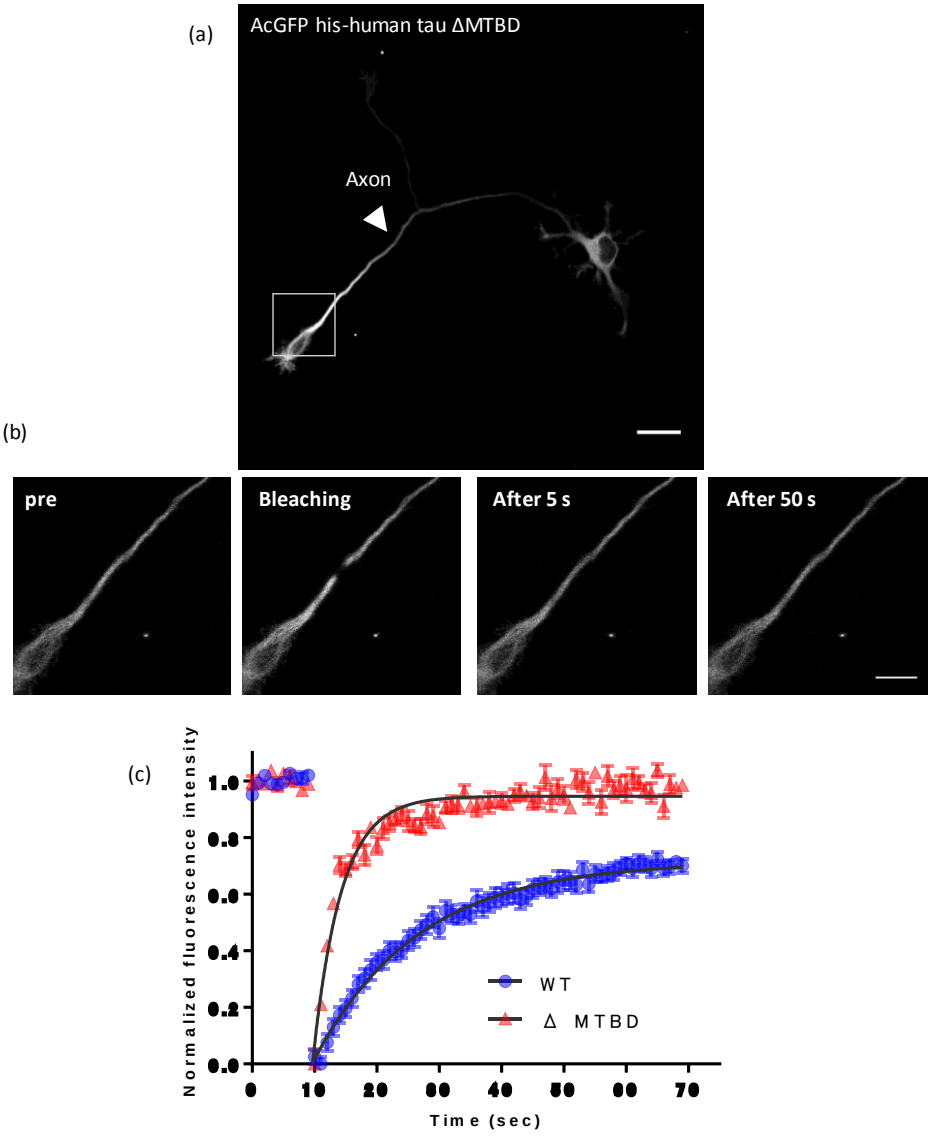

Fig. 24. **FRAP of ΔMTBD in the axon in stage 3 neurons at 3 DIV**
Recovery rate of fluorescence shown are the mean ± S.E.M (ΔMTBD n=8). The data of WT are from **Fig. 21**. Diffusion coefficient was shown in Table 5.

3.6. Investigating the potential transport mechanisms of tau

There must be a mechanism to localize ΔMTBD to the axon. One possible mechanism is that ΔMTBD is trapped in the axon, particularly near the tip where it accumulates most. I performed FRAP near the tip and a middle portion of the axon and compared fluorescence recovery (**Fig. 25**).

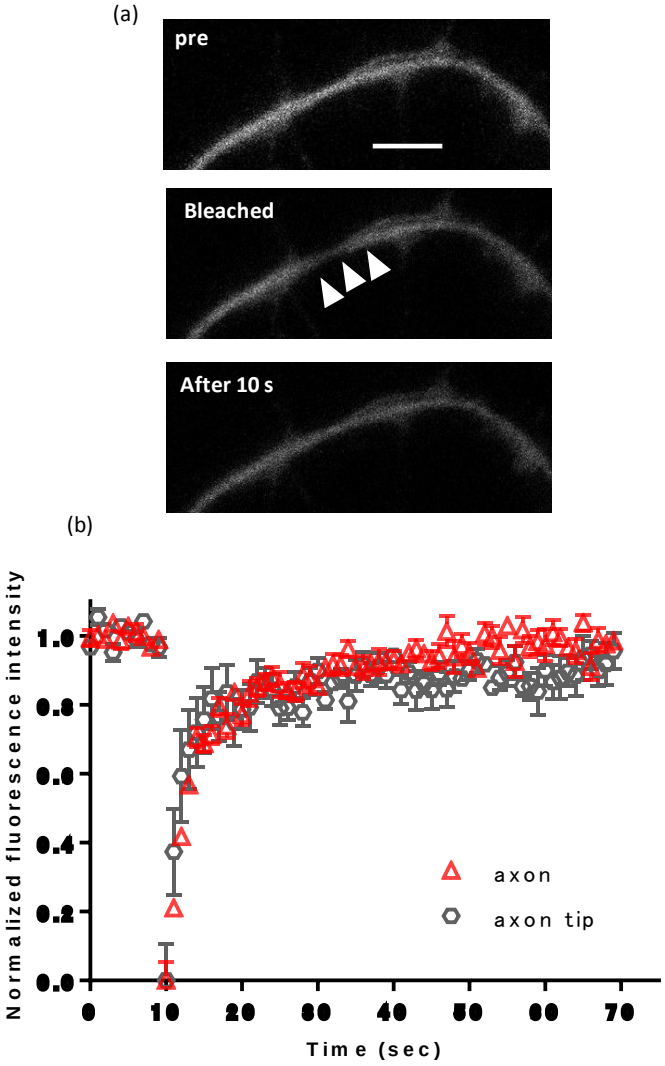

Fig. 25. **FRAP of ΔMTBD in the axon shaft and the tip**

FRAP was performed in the middle (**Fig. 24**) and near the tip (a) of the axon. Recovery rate of fluorescence of in a middle portion of the axon and the axon tip (b). Arrow head is the bleached area. Plots shown are the mean (n=4) ± S.E.M. Scale bar: 5 μm

I found that there were no significant differences in the mobility of ΔMTBD in the different parts of the axon. These results suggest that ΔMTBD moves almost freely and is not trapped in the axon.

The second possibility I considered was that a barrier like structure in the axon initial segment blocks tau, which once enters the axon, from going back to the soma, thereby resulting in the retention of tau in the axon. This is based on a previous study (Li et al., 2011). To test this, fluorescence in the entire soma and dendrites was bleached (**Fig. 26**). Then, I measured the recovery in the soma, of which fluorescent molecules must come from the axon. With the measurement in the axonal fluorescence decay adjacent to the bleached area, it is possible to know whether ΔMTBD can enter the soma from the axon and whether the barrier exists. After bleaching, the fluorescence intensity in the soma gradually recovered and reached at a constant level. Concomitantly, the fluorescence intensity in the axon decreased (**Fig. 26**). From these results, I concluded that ΔMTBD can move freely between the axon and the soma in these stage 3 neurons. Therefore, the "barrier" mechanism does not seem to be sufficient to account for the axonal localization of ΔMTBD.

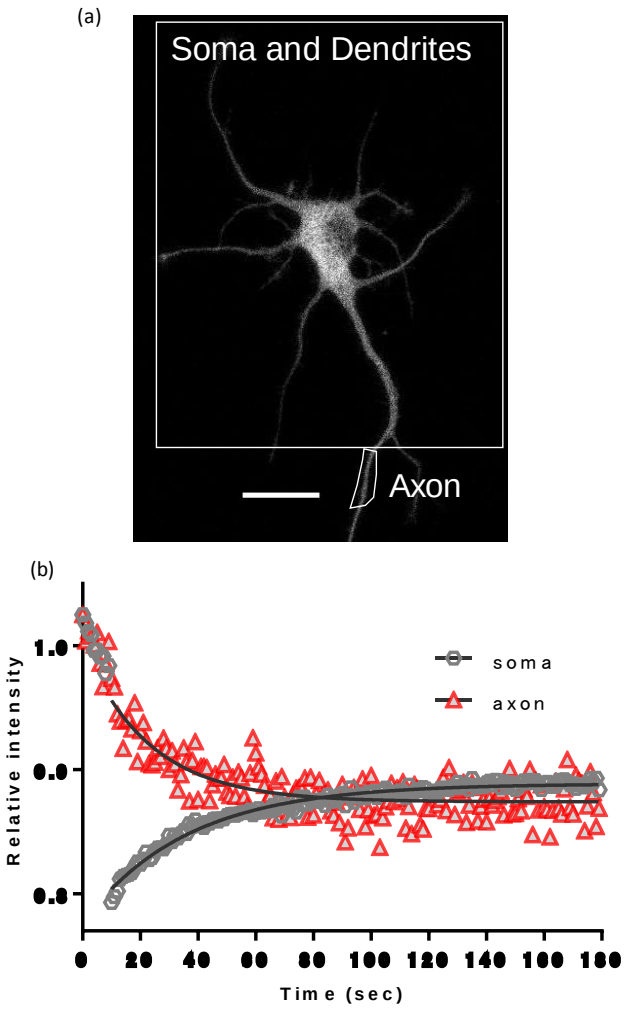

Fig. 26. **FRAP of ΔMTBD in the soma by recruiting axonal molecules**
FRAP was performed with a large bleaching area covering the entire somatodendritic region (a). Fluorescence signals were monitored in the soma and in the axon adjacent to the bleached area (b). Scale bar: 20 μm

As described earlier, I determined PRR2, instead of MTBD, as an important region using a series of deletion mutants for the axonal localization. ΔPRR2 distributed to the soma, dendrites and the axons of neurons (see **Figs. 16 and 17**). Because the results of ΔMTBD indicate that stable MT-binding is not necessary for axonal localization, it is possible that reinforced MT-binding is rather preventive of axonal localization. To test if ΔPRR2 binds more tightly to MTs than WT, I performed FRAP with this mutant. FRAP analysis of ΔPRR2 showed faster recovery than WT and slower recovery than ΔMTBD (**Fig. 27**). This is consistent with the in vitro MT-binding assay with ΔPRR2 (Iwata et al., 2019). These results again show the dissociation between MT-binding and axonal localization. Since ΔPRR2 did not show MT-binding capability above WT, I speculated that PRR2 may play an important role in the axonal transport of tau.

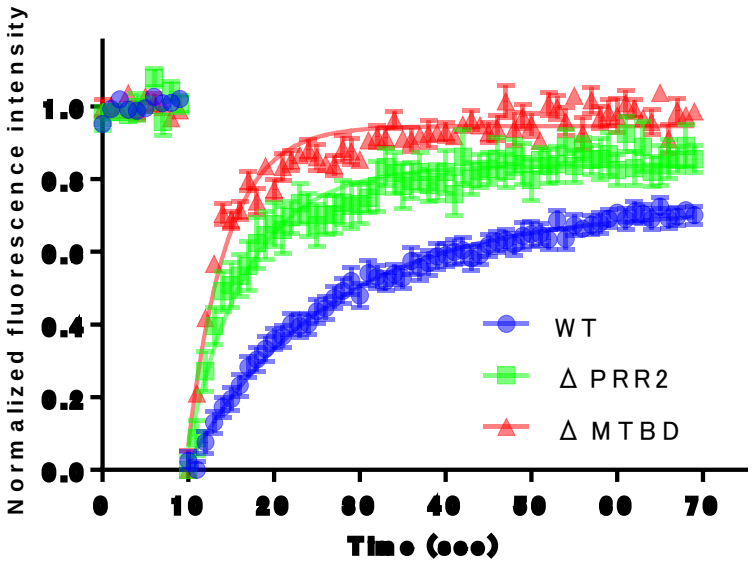

Fig. 27. **FRAP of ΔPRR2 in the axon in stage 3 neurons at 3 DIV**
Recovery of fluorescence shown is the mean ± S.E.M (ΔPRR2, n=11). The data of WT and ΔMTBD are from **Fig. 24**. Diffusion coefficient was shown in Table 5.

To test how tau is transported to the axon and if PRR2 is indeed important in this process, I performed FRAP with a large bleaching area at the base of the axon. This allowed me to evaluate how AcGFP-tau moves from the soma and from the distal end of the bleached area in the axon. Difference in the recovery rate between the somatic and axonal sides would indicate directional transport. The results of WT and ΔPRR2 are shown in **Fig. 28** and **Fig. 29**, respectively. In WT, the

recovery in the axonal side was slower than that in the somatic side (**Fig. 28**). This result indicates that tau is transported from the soma to distal axons beyond diffusion. I then examined ΔPRR2. Overall, the recovery of ΔPRR2 was faster than WT (**Fig. 29**), presumably due to its reduced binding to MTs. In contrast to WT, there was almost no difference in the recovery rate between these two sides for ΔPRR2. Therefore, I consider that the mobility of ΔPRR2 is dictated by diffusion and MT-binding but not directional transport. These results suggest that PRR2 is important in the axonal transport of tau from the soma in an early developmental stage.

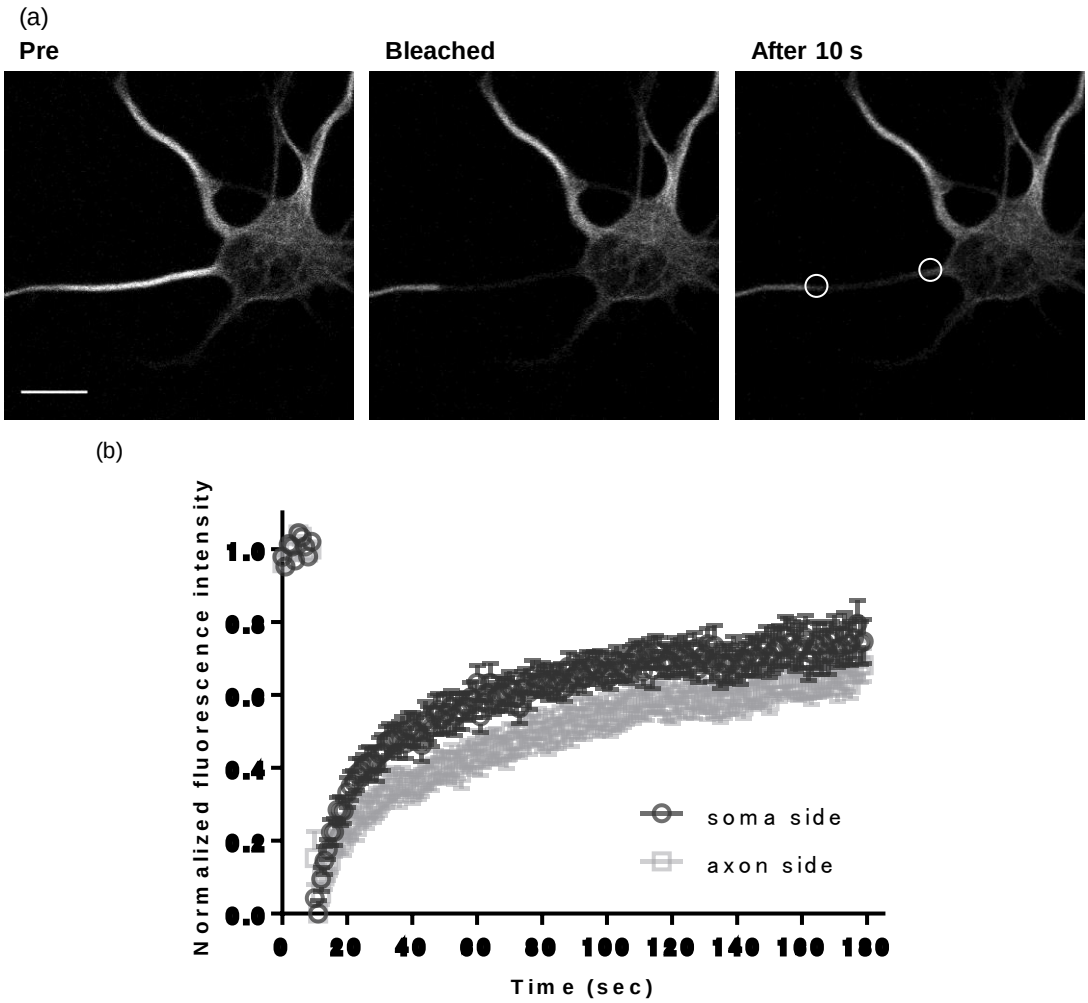

Fig. 28. **Asymmetric recovery of WT tau in the axon**

FRAP was performed in the initial part of the axon with a large bleached area (a). Images before, immediately after bleaching, and 10 s after bleaching are shown. Scale bar: 20 μm. Fluorescence recovery was monitored in the two ends of the bleached area indicated in (a), somatic and axonal sides (b). Recovery rates of fluorescence shown are the mean ± S.E.M (n=9).

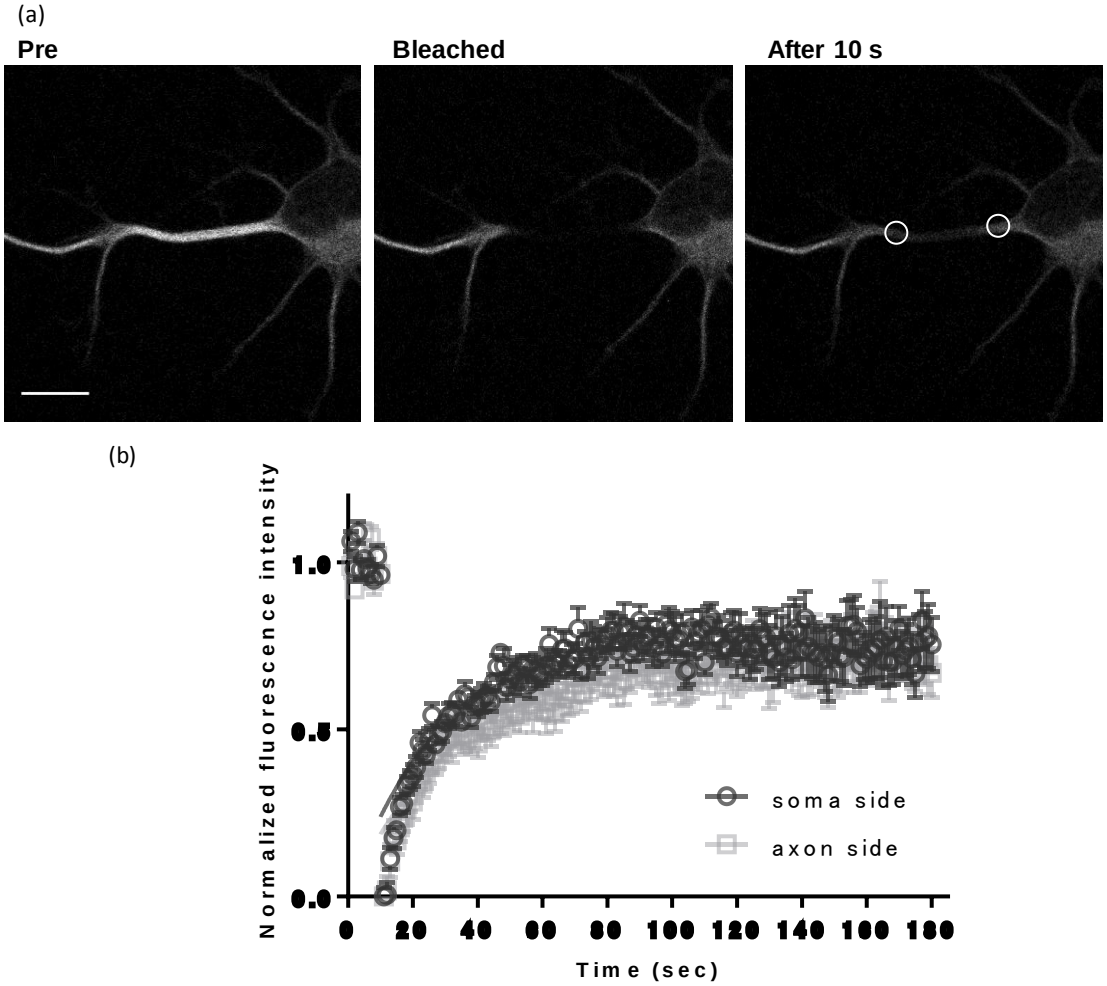

Fig. 29. **Symmetric recovery of ΔPRR2 in the axon**

FRAP was performed as in **Fig. 28** with ΔPRR2 (a). Scale bar: 20 μm. Recovery rates of fluorescence shown are the mean ± S.E.M (n=6) (b).

3.7. Phosphorylation and the axonal localization of tau

Tau is hyperphosphorylated in neurofibrillary tangles accumulated in the soma and dendrites. Therefore, it is possible that phosphorylation influences the localization of tau. There are eight known phosphorylation sites in PRR2 (**Fig. 30**). I made pseudo-phosphorylation (PRR2_8E) and pseudo-dephosphorylation (PRR2_8A) mutants with all eight sites substituted to either glutamate or alanine. These mutants were expressed with the inducible expression method and analyzed for their localization and mobility at 3 DIV.

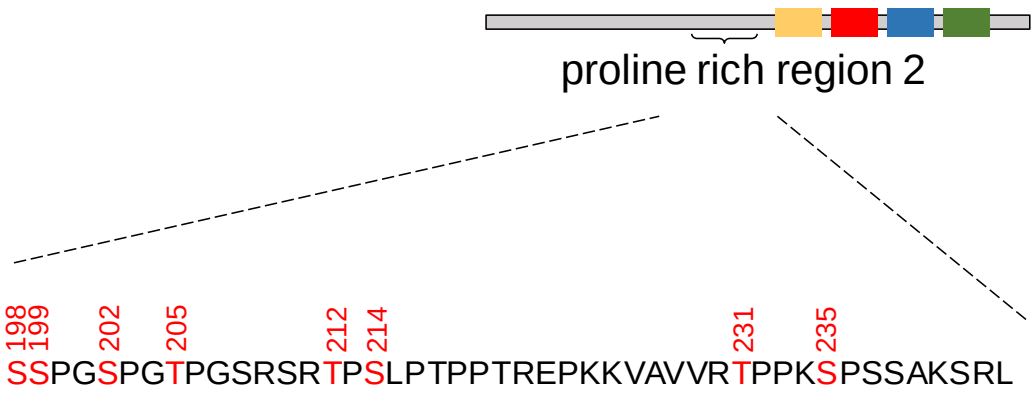

Fig. 30. **Phosphorylation sites of tau in PRR2**
Amino acid sequence of PRR2. The red letters indicate the eight putative phosphorylation sites mutated to Ala (PRR2_8A) or mutated to Glu (PRR2_8E). The numbering is based on the 2N4R isoform of human tau.

I found that both of the mutants showed distributions different from that of WT. They both show more accumulations in the soma and dendrites than WT. This was also reflected in the different axon/dendrite ratios, which was significantly less than WT and similar to that of ΔPRR2 (**Fig. 31, 32, 33**). Therefore, phosphorylation and dephosphorylation of PRR2 can impact the localization of tau in neurons.

(a)

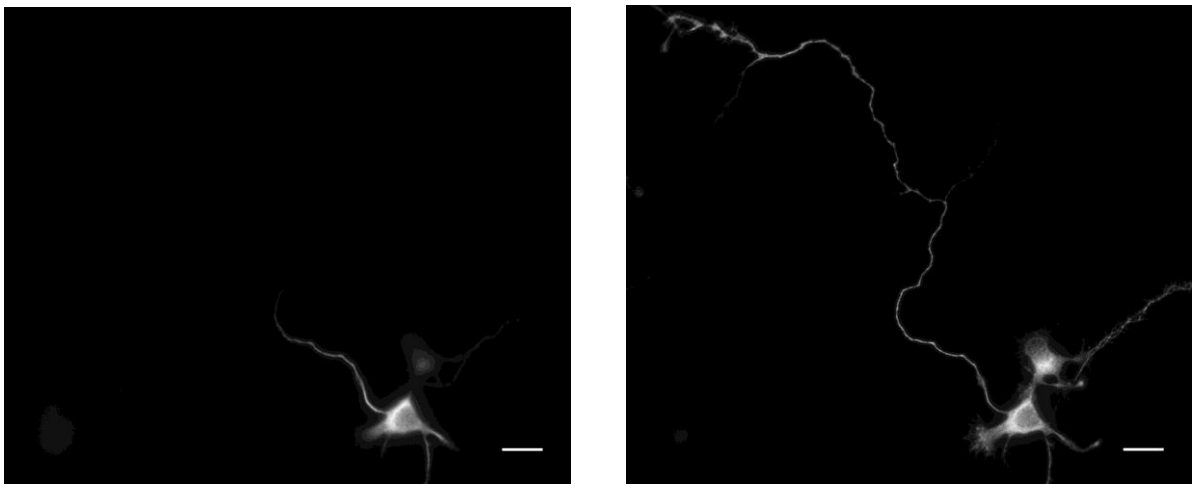
Human tau PRR2_8A
Endogenous Tau

(b)

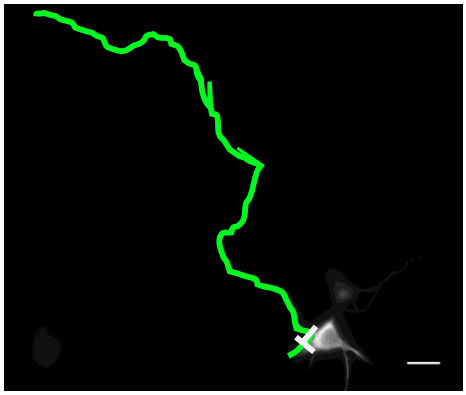

(c)

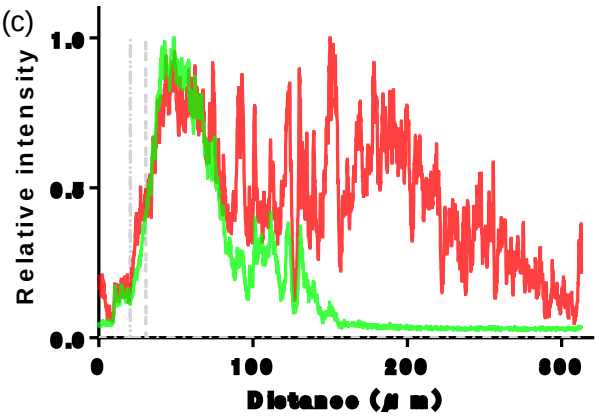
Relative intensity
1.0
0.5
0.0
0
100
200
300
Distance (μm)

(d)

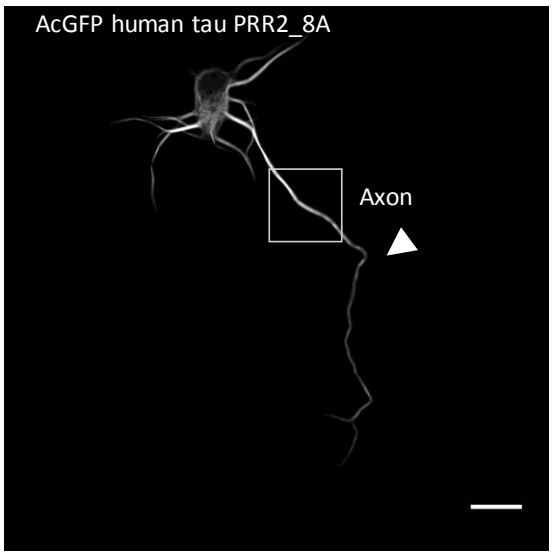
AcGFP human tau PRR2_8A
Axon

(e)

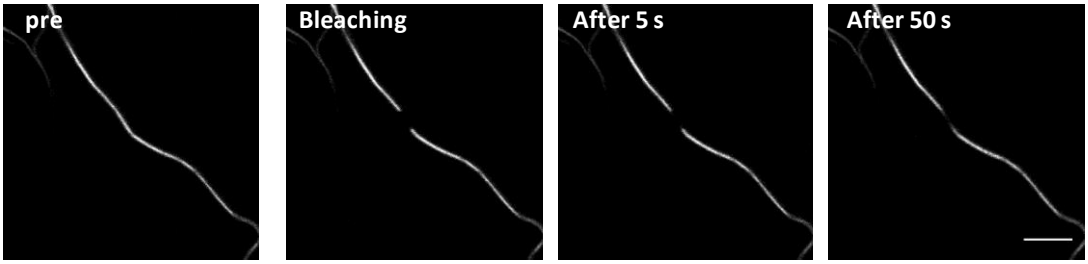
pre
Bleaching
After 5 s
After 50 s

Fig. 31. **Localization and FRAP of tau PRR2_8A at 3 DIV**

Neurons incubated with doxycycline at 1 DIV were fixed at 3 DIV and immunostained for endogenous tau (red) and PRR2_8A (green). Signal intensities were adjusted to have similar intensities in the axon. PRR2_8A was retained drastically in the soma and dendrites (a). Scale bars: 20 µm. Line scan analysis of PRR2_8A and endogenous tau from a neurite through the soma and to the distal tip of the axon (b). The intensity peak of PRR2_8A appeared in the soma, instead of the distal axon (c). The vertical dotted lines indicate the borders between the neurite and the soma and between the soma and the axon. Direct fluorescence image of a representative neuron used for FRAP is shown in (d). FRAP was performed in a middle portion in the boxed area in (d). Images before, immediately after bleaching, and 5 s and 50 s after bleaching are shown (e). Scale bars: 20 µm (d), 10 µm (e).

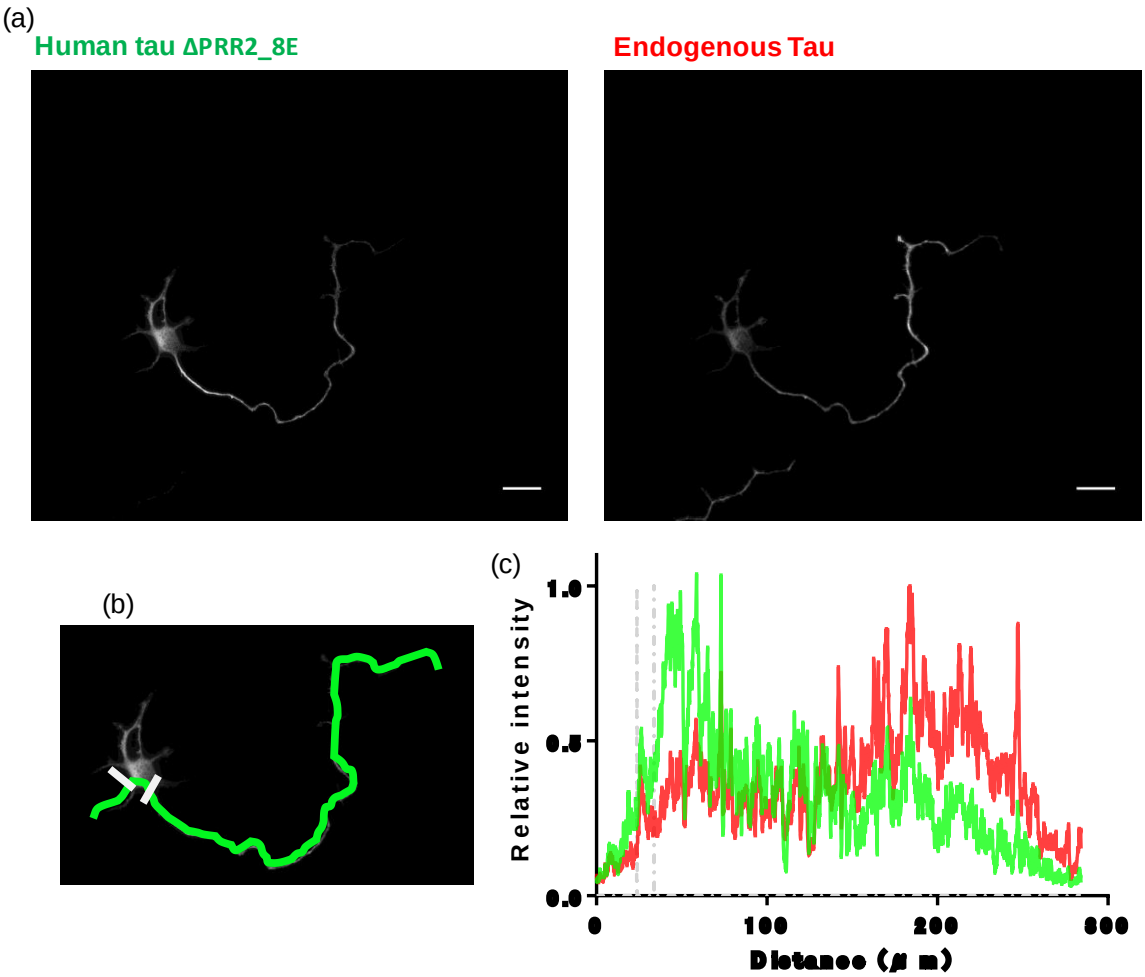
(a)
Human tau ΔPRR2_8E
Endogenous Tau
(b)
(c)
Relative intensity
1.0
0.5
0.0
0
100
200
300
Distance (μm)
(d)
AcGFP his-human tau PRR2_8E
Axon
(e)
pre
Bleaching
After 5 s
After 50 s

Fig. 32. **Localization and FRAP of tau PRR2_8E at 3 DIV**

Neurons incubated with doxycycline at 1 DIV were fixed at 3 DIV and immunostained for endogenous tau (red) and PRR2_8E (green). Signal intensities were adjusted to have similar intensities in the axon. Like WT (Fig. 15), PRR2_8E was retained in the soma and dendrites (a). Scale bars: 20 µm. Line scan analysis of PRR2_8E tau and endogenous tau from a neurite through the soma and to the distal tip of the axon (b). The intensity peak of PRR2_8E tau appeared in the soma, instead of the distal axon (c). The vertical dotted lines indicate the borders between the neurite and the soma and between the soma and the axon. Direct fluorescence image of a representative cell used for FRAP is shown in (d). FRAP was performed in a middle portion of the axon. Images before, immediately after bleaching, and 5 s and 50 s after bleaching are shown (e). Scale bars: 20 µm (d), 10 µm (e).

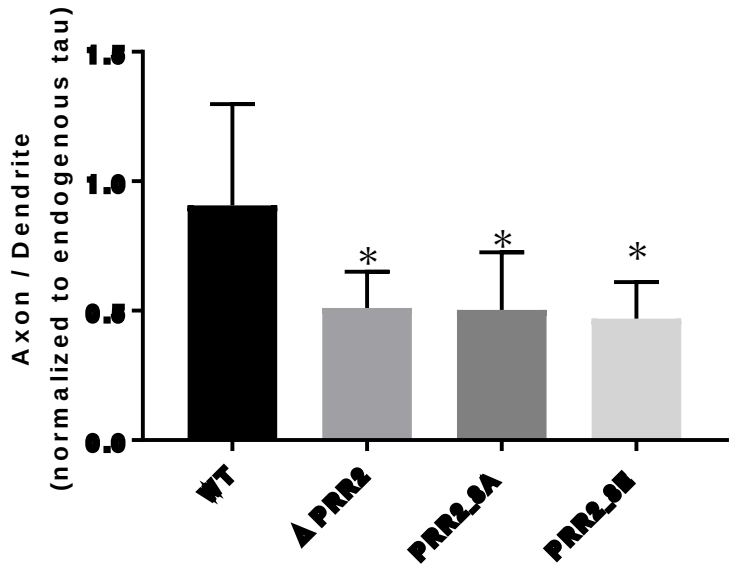

Fig. 33. **Localization of PRR2_8A and PRR2_8E in stage 3 neurons**

Quantification of how exogenous tau is enriched in the axon using the ratio of axonal signals over dendritic signals normalized to those of endogenous tau as shown in Fig. 17. Endogenous tau, exogenous tau (WT ΔPRR2, PRR2_8A and PRR2_8E) were compared. Colocalization of exogenous tau and endogenous tau would show a value close to 1. WT : n=7, ΔPRR2 : n=9, PRR2_8A : n=7, PRR2_8E : n=4. *p= 0.113 (ΔPRR2), 0.0151 (PRR2_8A), 0.0197 (PRR2_8E) using ANOVA with Dunnett's post hoc tests.

FRAP analysis revealed that the recovery of PRR2_8E was faster than WT and comparable to ΔPRR2 (**Fig. 34**). This is consistent with the in vitro MT-binding assay (Iwata et al., 2019). In contrast, the recovery of PRR2_8A was dramatically slowed (**Fig. 34**), showing its tight and stable binding to MTs. Therefore, tight binding to MTs prevents PRR2_8A from being efficiently transported to the axon, thereby trapping it in the soma. Regarding PRR2_8E, because the phenotype (localization and MT-binding) is quite similar to that of ΔPRR2, I speculate that that phosphorylation of PRR2 on the 8 sites inhibits the activity of PRR2 on tau transport like the deletion of PRR2 itself. Taken together, these results suggest that phosphorylation of PRR2 can regulate MT-binding and transport of tau independently.

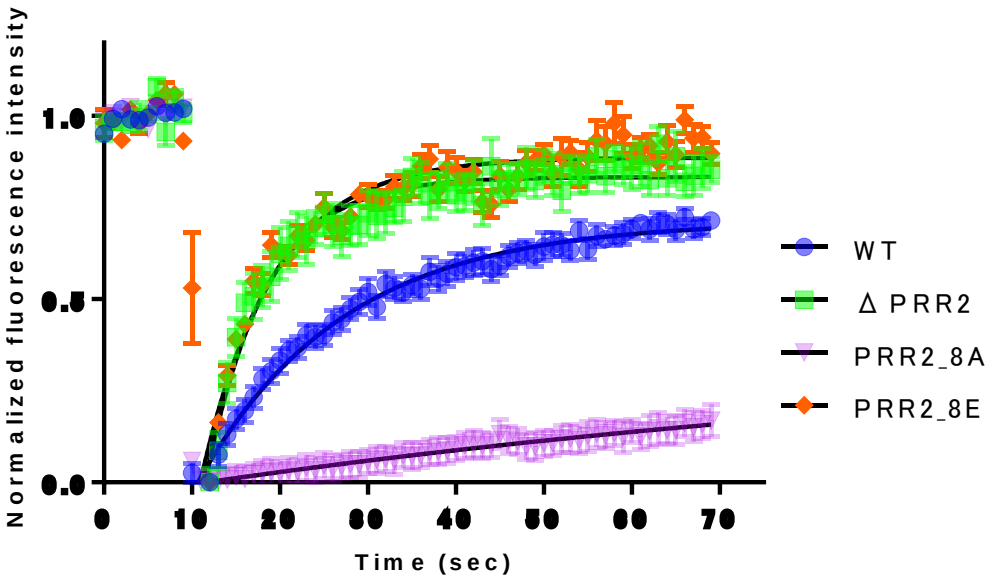

Fig. 34. **The mobility of PRR2_8A and PRR2_8E in the axons in stage 3 neurons at DIV 3**
Comparing of WT, ΔPRR2, PRR2_8A and PRR2_8E in the axon at DIV 3. Recovery rates of fluorescence shown are the mean ± S.E.M (PRR2_8A : n=7, PRR2_8E : n=7). The data of WT are from Fig. 21. Diffusion coefficients are shown in Table 5.

Table 5. Diffusion coefficient of each tau at DIV 3

	D (μm^2/s)
WT	0.172±0.0148
ΔPRR2	0.406±0.0706
ΔMTBD	0.624±0.0736
PRR2_8A	N.D.
PRR2_8E	0.338±0.398

The diffusion coefficients were computed using the one-dimensional diffusion equation (1).

$$D=\omega^2/4TD \qquad (1)$$

4. DISCUSSION

In this thesis research, I established a new experimental method to study mechanisms for the axonal localization of tau in neurons. In contrast to conventional expression methods, in which human tau is constitutively expressed by transfection and a strong promoter in relatively mature neurons, the new method uses a lentiviral vector and an inducible expression system to express human tau transiently in immature neurons. This was based on the finding that endogenous tau is highly expressed during early development, and that the axonal localization occurs at early stages as well (Kubo et al., 2019b). Using this method as an experimental model system, I obtained a number of new findings regarding how tau localizes to the axon. I believe that this new expression method will be useful for studying tau localization and mis-localization in the future.

4.1. Axonal localization of tau is related to the timing of expression

The new method allows for axon specific localization of exogenous tau by expressing it transiently and during the early developmental stages of neuron. Previous studies found that tau mRNA expression is high during the first week of postnatal development and declines significantly after that in mice (Kubo et al., 2019b). Human tau expressed beyond the developmental period mis-localizes to the soma and dendrites in tau transgenic mice (Kubo et al., 2019b). In contrast, human tau expressed in the same manner as endogenous tau results in its axonal localization in knock-in mice. These are consistent with my findings that human tau expressed in stage 4 neurons at 7 DIV constitutively did not show axon-specific localization. Taken together, these findings demonstrate the importance of the expression timing and pattern for the axon-specific localization of tau.

It is possible that the level of exogenous tau expressed at 7 DIV is simply higher than that induced at 1 DIV. The excess level of exogenous tau beyond endogenous tau may overwhelm the transport machinery and mis-localize. Although I cannot exclude this possibility, my FRAP experiments indicate that developmental changes in MT-binding is the key. I found in the FRAP experiments that the dephosphorylation-mimetic mutant (PRR2_8A) bound to MTs tightly and was

accumulated in the soma (**Fig. 31**). These results suggest that tight MT-binding in the soma could prevent tau from being transported to the axon. Since FRAP analyses suggested that MT-binding of tau in the soma becomes more stable during neuronal maturation (**Fig. 23**), exogenous tau expressed in mature neurons is prone to be trapped in the soma. It may also be possible that the transport system of tau works more efficiently in immature neurons (stage 3 neurons) than more mature neurons (stage 4 neurons), as tau localization occurs actively in early development in vivo (Kubo et al., 2019b) and in culture (this study). So, when exogenous tau misses the right timing for expression, it tends to remain in the soma and dendrites. These two possibilities may explain why tau expressed in stage 4 neurons mis-localizes. These findings also tell us that, when investigating the localization mechanism of a protein, knowing the expression pattern of the endogenous protein and mimicking it may provide new insights into the mechanism.

4.2. Phosphorylation regulates the localization and MT-binding of tau

Tau has been known as a protein highly phosphorylated in developing brains and in AD patient brains. It has also been known that tau is highly phosphorylated at PRR2 in these conditions (Wang and Mandelkow, 2016). Particularly, phosphorylation of Ser202 and Thr205 is specific to aggregated tau in AD and the epitope of the AT8 antibody. It should also be noted that four phosphorylation sites (Ser195, Ser198, Ser199, and Ser202) are the putative epitope of the tau-1 antibody. In the deletion mutant experiments, PRR2 was found to be important for the axonal localization of tau. Therefore, I investigated whether PRR2 phosphorylation affects the axonal localization by using phosphorylation-mimetic and dephosphorylation-mimetic mutants for all eight putative phosphorylation sites in PRR2. Since PRR2 has also been implicated in MT-binding (Kiris et al., 2011; Schwalbe et al., 2015), I also examined these mutants in the FRAP experiments.

The results indicated that PRR2 phosphorylation regulates the localization. As discussed above, the dephosphorylation-mimetic mutant (PRR2_8A) showed greatly reduced mobility in FRAP, showing its tight binding to MTs. This mutant accumulated in the soma, presumably due to its tight

binding to somatic MTs. In contrast, the phosphorylation-mimetic mutant (PRR2_8E) showed lower MT-binding than WT (**Fig. 32**). These results indicate that phosphorylation of PRR2 regulates MT-binding bidirectionally. WT tau showed an intermediate MT-binding between PRR2_8A and PRR2_8E. Therefore, WT tau must be phosphorylated at a certain level in situ to reduce MT-binding in immature neurons, which is consistent with the fact that tau is highly phosphorylated in developing brains (Wang and Mandelkow, 2016). This may facilitate the transport of tau from the soma to the axon in immature neurons (stage 3 neurons), as ΔMTBD efficiently localized to the axon.

However, PRR2_8E mis-localized, although it showed less MT-binding than WT. My results suggested that PRR2 is important for not only MT-binding but also axonal transport of tau. Therefore, phosphorylation of all sites on PRR2 may inhibit the transport like the deletion. I speculate that for tau to be transport to the axon, certain sites on PRR2 need to be phosphorylated to be free from somatic MTs, and the other sites need to stay dephosphorylated to engage with the transport mechanism (**Fig. 35**). In future research, each phosphorylation site should be mutated individually to determine which sites regulate MT-binding and axonal transport.

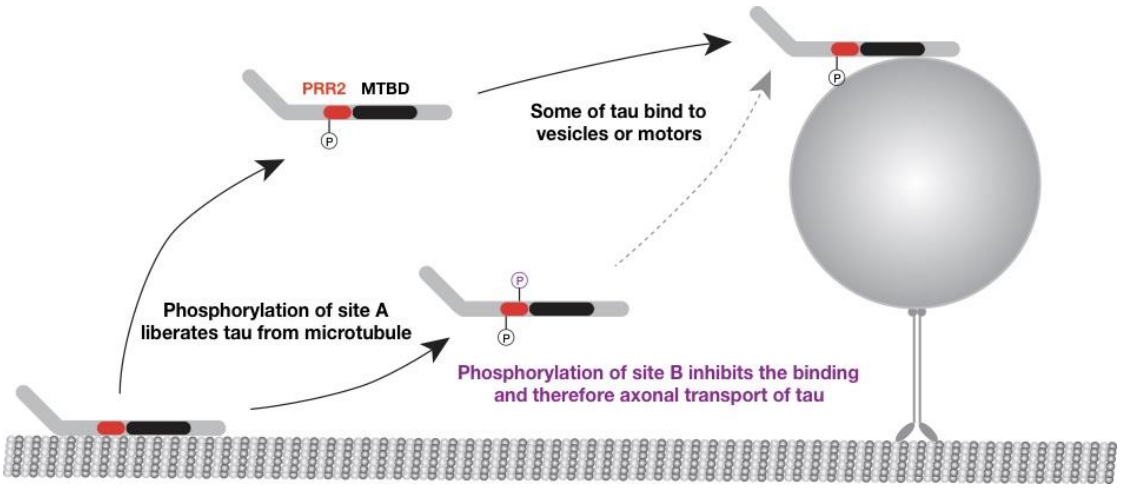

Fig. 35. **Regulation of MT-binding and transport of tau through phosphorylation**
The results of PRR2_8A suggest that complete dephosphorylation of PRR2 would results in stable MT-binding and trapping of tau in the soma. Tau needs to be liberated from somatic MTs by phosphorylation of the putative site A. Complete phosphorylation of PRR2 (PRR2_8E) could reduce MT-binding. However, it also prevents tau from being transported by the slow axonal transport mechanism. This mechanism is not known, but piggybacking the fast axonal transport has been proposed as a candidate mechanism (Roy, 2014).

4.3. The localization mechanism of tau

The results from FRAP experiments suggest that ΔMTBD is not trapped or anchored in distal dendrites. Also, there does not seem to be physical barriers to prevent ΔMTBD to go back from the axon to the soma. These mechanisms are not necessary at least for ΔMTBD. The FRAP results of WT and ΔPRR2 indicate that there is a PRR2-dependent transport mechanism for tau to the axon. In fact, tau has been shown to be transported by the slow axonal transport with other cytoplasmic and soluble proteins (Tytell et al., 1984; Mercken et al., 1995; Tashiro et al., 1996). Previous studies have suggested that tau is transported by MT-dependent mechanisms (Utton et al., 2005; Falzone et al., 2009; Scholz and Mandelkow, 2014). My result of ΔMTBD is not consistent with these studies and surprising. Currently, the mechanisms of slow axonal transport and of tau transport are not known. I believe the experimental system I established in this thesis research will provide a useful tool to study not only tau transport mechanism but also the enigmatic slow axonal transport mechanisms.

4.4. Implications in AD pathology

In this thesis study, I found that the axonal localization of tau completes during the early developmental period and that tau expressed beyond this period mis-localizes. This is consistent with the previous report that tau expression is largely limited during the perinatal period (Kubo et al., 2019b). Based on these findings, I hypothesize that the production of tau protein and its axonal localization occur mostly only during the perinatal development, such that tau excessively expressed beyond this period would mis-localize. From this, I speculate that tau is ectopically expressed during the pathogenesis of AD in adult mature neurons and therefore mis-localized and hyper-phosphorylated. The ectopic expression in AD needs to be investigated to support this hypothesis. Also, future experiments investigating if the pathology could be reproduced in cultured cells would help examining the possibility.

5. REFERENCE

Akhmanova A and Hoogenraad CC (2005) Microtubule plus-end-tracking proteins: mechanisms and functions. Current Opinion in Cell Biology, 17:47–54

Arimura N, Kaibuchi K (2007) Neuronal polarity: from extracellular signals to intracellular mechanisms. Nat Rev Neurosci, 8:194–205.

Avila J (2008) Tau kinases and phosphatases. J. Cell. Mol. Med. Vol 12, No 1, pp. 258-259

Barbier P, Zejneli O, Martinho M, Lasorsa A, Belle V, Smet-Nocca C, Tsvetkov PO, Devred F, Landrieu I (2019) Role of Tau as a Microtubule-Associated Protein: Structural and Functional Aspects. Front Aging Neurosci, 11:204.

Cummings JL, Greg Cole G (2002) Alzheimer Disease. JAMA. Vol 287, No. 18, 2335-2338

Curcio M, Bradke F (2015) Microtubule Organization in the Axon: TRIM46 Determines the Orientation. Neuron, 88:1072–1074.

Dotti CG, Sullivan CA, and Banker GA (1988) The Establishment of Polarity by Hippocampal Neurons in Culture. The Journal of Neuroscience, 8(4): 1454-l 488

Decker JM, Krüger L, Sydow A, Zhao S, Frotscher M, Mandelkow E, Mandelkow EM (2015) Pro-aggregant Tau impairs mossy fiber plasticity due to structural changes and Ca(++) dysregulation. Acta Neuropathol Commun, 3:23

Dehmelt L and Halpain S (2004) The MAP2/Tau family of microtubule-associated proteins. *Genome Biology*, Volume 6, Issue 1, Article 204: 204.1-204.10

Delacourte A, David JP, Sergeant N, Buée L, Wattez A, Vermersch P, Ghozali F, Fallet-Bianco C, Pasquier F, Lebert F, Petit H, Di Menza C (1999) The biochemical pathway of neurofibrillary degeneration in aging and Alzheimer's disease. Neurology, 52:1158–1165.

Falzone TL, Stokin GB, Lillo C, Rodrigues EM, Westerman EL, Williams DS, Goldstein LS (2009) Axonal stress kinase activation and tau misbehavior induced by kinesin-1 transport defects. J Neurosci, 29:5758–5767.

Ghetti B, Oblak AL, Boeve BF, Johnson KA, Dickerson BC, Goedert M (2015) Invited review: Frontotemporal dementia caused by microtubule-associated protein tau gene (MAPT) mutations:

a chameleon for neuropathology and neuroimaging. Neuropathol Appl Neurobiol, 41:24–46

Gómez-Isla T, Hollister R, West H, Mui S, Growdon JH, Petersen RC, Parisi JE, Hyman BT (1997) Neuronal loss correlates with but exceeds neurofibrillary tangles in Alzheimer's disease. Ann Neurol, 41:17–24.

Inagaki N, Chihara K, Arimura N, Ménager C, Kawano Y, Matsuo N, Nishimura T, Amano M, Kaibuchi K (2001) CRMP-2 induces axons in cultured hippocampal neurons. Nat Neurosci, 4:781–782.

Iwata M, Watanabe S, Yamane A, Miyasaka T, Misonou H (2019) Regulatory mechanisms for the axonal localization of tau protein in neurons. Mol Biol Cell, 30:2441–2457.

Jensen CS, Watanabe S, Stas JI, Klaphaak J, Yamane A, Schmitt N, Olesen SP, Trimmer JS, Rasmussen HB, Misonou H (2017) Trafficking of Kv2.1 Channels to the Axon Initial Segment by a Novel Nonconventional Secretory Pathway. J Neurosci, 37:11523–11536.

Kaech S and Banker G (2006) Culturing hippocampal neurons. Nature Protocols, vol.1 no.5, 2406-2415.

Kanai Y, Chen J and Hirokawa N (1992) Microtubule bundling by tau proteins in vivo: analysis of functional domains. The EMBO Journal vol.1 1 no.1 1 pp.3953-3961.

Kanai Y, Hirokawa N (1995) Sorting mechanisms of tau and MAP2 in neurons: suppressed axonal transit of MAP2 and locally regulated microtubule binding. Neuron, 14:421–432.

Kiris E, Ventimiglia D, Sargin ME, Gaylord MR, Altinok A, Rose K, Manjunath BS, Jordan MA, Wilson L, Feinstein SC (2011) Combinatorial Tau pseudophosphorylation: markedly different regulatory effects on microtubule assembly and dynamic instability than the sum of the individual parts. J Biol Chem, 286:14257–14270.

Kneynsberg A, Combs B, Christensen K, Morfini G, Kanaan NM (2017) Axonal Degeneration in Tauopathies: Disease Relevance and Underlying Mechanisms. Frontiers in neuroscience 11:572.

Kubo A, Misonou H, Matsuyama M, Nomori A, Wada-Kakuda S, Takashima A, Kawata M, Murayama S, Ihara Y, Miyasaka T (2019) Distribution of endogenous normal tau in the mouse

brain. J Comp Neurol, 527:985–998.

Kubo A, Ueda S, Yamane A, Wada-Kakuda S, Narita M, Matsuyama M, Nomori A, Takashima A, Kato T, Onodera O, Goto M, Ito M, Tomiyama T, Mori H, Murayama S, Ihara Y, Misonou H, Miyasaka T (2019) Ectopic expression induces abnormal somatodendritic distribution of tau in the mouse brain. Journal of Neuroscience, 39 (34) 6781-6797.

Li X, Kumar Y, Zempel H, Mandelkow EM, Biernat J, Mandelkow E (2011) Novel diffusion barrier for axonal retention of Tau in neurons and its failure in neurodegeneration. EMBO J, 30:4825–4837.

Mandell JW, Banker GA (1996) A spatial gradient of tau protein phosphorylation in nascent axons. J Neurosci, 16:5727–5740.

Mercken M, Fischer I, Kosik KS, Nixon RA (1995) Three distinct axonal transport rates for tau, tubulin, and other microtubule-associated proteins: evidence for dynamic interactions of tau with microtubules in vivo. J Neurosci, 15:8259–8267.

Mietelska-Porowska A, Wasik U, Goras M, Filipek A and Niewiadomska G (2014) Tau Protein Modifications and Interactions: Their Role in Function and Dysfunction. Int. J. Mol. Sci., 15, 4671-4713

Misonou H, and Trimmer JS (2005) A primary culture system for biochemical analyses of neuronal proteins. Journal of Neuroscience Methods 144 165–173.

Ono M, Sahara N, Kumata K, Ji B, Ni R, Koga S, Dickson DW, Trojanowski JQ, Lee VM, Yoshida M, Hozumi I, Yoshiyama Y, van Swieten JC, Nordberg A, Suhara T, Zhang MR, Higuchi M (2017) Distinct binding of PET ligands PBB3 and AV-1451 to tau fibril strains in neurodegenerative tauopathies. Brain : a journal of neurology 140:764-780.

Qiang L, Sun X, Austin TO, Muralidharan H, Jean DC, Liu M, Yu W, Baas PW (2018) Tau Does Not Stabilize Axonal Microtubules but Rather Enables Them to Have Long Labile Domains. Curr Biol, 28:2181–2189.e4.

Roy S (2014) Seeing the unseen: the hidden world of slow axonal transport. Neuroscientist,

20:71–81.

Scholz T and Mandelkow E (2014) Transport and diffusion of Tau protein in neurons. Cell Mol Life Sci, 71:3139–3150.

Song AH, Wang D, Chen G, Li Y, Luo J, Duan S, Poo MM (2009) A selective filter for cytoplasmic transport at the axon initial segment. Cell, 136:1148–1160.

Schwalbe M, Kadavath H, Biernat J, Ozenne V, Blackledge M, Mandelkow E, Zweckstetter M (2015) Structural Impact of Tau Phosphorylation at Threonine 231. Structure, 23:1448–1458.

Szendrei GI, Lee VM, Otvos L (1993) Recognition of the minimal epitope of monoclonal antibody Tau-1 depends upon the presence of a phosphate group but not its location. J Neurosci Res, 34:243–249.

Tashiro T, Sun X, Tsuda M, Komiya Y (1996) Differential axonal transport of soluble and insoluble tau in the rat sciatic nerve. J Neurochem, 67:1566–1574.

Tomba C (2015) Primary brain cells in in vitro controlled microenvironments : single cell behaviors for collective functions. HAL

Tourtellotte WG, Van Hoesen GW (1991) The axonal origin of a subpopulation of dystrophic neurites in Alzheimer's disease. Neurosci Lett, 129:11–16.

Tytell M, Brady ST, Lasek RJ (1984) Axonal transport of a subclass of tau proteins: evidence for the regional differentiation of microtubules in neurons. Proc Natl Acad Sci U S A, 81:1570–1574.

Utton MA, Noble WJ, Hill JE, Anderton BH, Hanger DP (2005) Molecular motors implicated in the axonal transport of tau and alpha-synuclein. J Cell Sci, 118:4645–4654.

Valiron O, Caudron N and Job D (2001) Microtubule dynamics. CMLS, Cell. Mol. Life Sci. 58 2069–2084

Van Beuningen SF, Will L, Harterink M, Chazeau A, Van Battum EY, Frias CP, Franker MA, Katrukha EA, Stucchi R, Vocking K, Antunes AT, Slenders L, Doulkeridou S, Sillevis Smitt P, Altelaar AF, Post JA, Akhmanova A, Pasterkamp RJ, Kapitein LC, De Graaff E, Hoogenraad CC

et al. (2015) TRIM46 Controls Neuronal Polarity and Axon Specification by Driving the Formation of Parallel Microtubule Arrays. Neuron, 88:1208–1226.

Voelzmann A, Hahn I, Pearce SP, Sánchez-Soriano N, Prokop A (2016) A conceptual view at microtubule plus end dynamics in neuronal axons. Brain Research Bulletin 126, 226–237

Wang Y, Mandelkow E (2016) Tau in physiology and pathology. Nat Rev Neurosci, 17:5–21.

Weissmann C, Reyher HJ, Gauthier A, Steinhoff HJ, Junge W, Brandt R (2009) Microtubule binding and trapping at the tip of neurites regulate tau motion in living neurons. Traffic, 10:1655–1668.

Xia D, Gutmann JM, Götz J (2016) Mobility and subcellular localization of endogenous, gene-edited Tau differs from that of over-expressed human wild-type and P301L mutant Tau. Sci Rep, 6:29074.